Sexual Dichromatism Drives Diversification Within a Major Radiation of African Amphibians

Daniel M. Portik[1,2*], Rayna C. Bell[2,3], David C. Blackburn[4], Aaron M. Bauer[5], Christopher D. Barratt[6,7,8], William R. Branch[9,10], Marius Burger[11,12], Alan Channing[13], Timothy J. Colston[14,15], Werner Conradie[9,16], J. Maximillian Dehling[17], Robert C. Drewes[18], Raffael Ernst[19, 20], Eli Greenbaum[21], Václav Gvoždík[22,23], James Harvey[24], Annika Hillers[25,26], Mareike Hirschfeld[25], Gregory F.M. Jongsma[4], Jos Kielgast[27], Marcel T. Kouete[4], Lucinda P. Lawson[28,29], Adam D. Leaché[30], Simon P. Loader[31], Stefan Lötters[32], Arie van der Meijden[33], Michele Menegon[34], Susanne Müller[32], Zoltán T. Nagy[35], Caleb Ofori-Boateng[36], Annemarie Ohler[37], Theodore J. Papenfuss[2], Daniela Rößler[32], Ulrich Sinsch[17], Mark-Oliver Rödel[25], Michael Veith[32], Jens Vindum[18], Ange-Ghislain Zassi-Boulou[38], and Jimmy A. McGuire[2]

[1]*Department of Ecology and Evolutionary Biology, University of Arizona, Tucson, Arizona 85721 USA*

[2]*Museum of Vertebrate Zoology, University of California, Berkeley, California 94720, USA*

[3]*Department of Vertebrate Zoology, National Museum of Natural History, Smithsonian Institution, Washington, DC 20560-0162 USA*

[4]*Florida Museum of Natural History, University of Florida, Gainesville, Florida 32611, USA*

[5]*Department of Biology, Villanova University, 800 Lancaster Avenue, Villanova, Pennsylvania 19085, USA*

[6]*Department of Environmental Sciences, University of Basel, Basel 4056, Switzerland*

[7]*German Centre for Integrative Biodiversity Research (iDiv) Halle-Jena-Leipzig, 0413 Leipzig, Germany*

[8]*Max Planck Institute for Evolutionary Anthropology, 0413 Leipzig, Germany*

[9]*Port Elizabeth Museum, P.O. Box 11347, Humewood 6013, South Africa*

[10]*Department of Zoology, P.O. Box 77000, Nelson Mandela Metropolitan University, Port Elizabeth 6031, South Africa*

[11]*African Amphibian Conservation Research Group, Unit for Environmental Sciences and Management, North-West University, Potchefstroom 2520, South Africa*

[12]*Flora Fauna & Man, Ecological Services Ltd. Tortola, British Virgin Island*

[13]*Unit for Environmental Sciences and Management, North-West University, Potchefstroom 2520, South Africa*

[14]*Department of Biological Sciences, Florida State University, Tallahassee, FL 32306, USA*

[15]*Zoological Natural History Museum, Addis Ababa University, Arat Kilo, Addis Ababa, Ethiopia*

[16]*School of Natural Resource Management, George Campus, Nelson Mandela University, George 6530, South Africa*

[17]*Institute of Sciences, Department of Biology, University of Koblenz-Landau, Universitätsstr. 1, D-56070 Koblenz, Germany*

[18]*California Academy of Sciences, San Francisco, California 94118, USA*

[19]*Museum of Zoology, Senckenberg Natural History Collections Dresden, Königsbrücker Landstr. 159, 01109 Dresden, Germany*

[20]*Department of Ecology, Technische Universität Berlin, Rothenburgstr. 12, 12165 Berlin, Germany*

[21]*Department of Biological Sciences, University of Texas at El Paso, El Paso, TX 79968, USA*

[22]*The Czech Academy of Sciences, Institute of Vertebrate Biology, Brno, Czech Republic*

[23]*National Museum, Department of Zoology, Prague, Czech Republic*

[24]*Pietermaritzburg, KwaZulu-Natal, South Africa*

[25]*Museum für Naturkunde, Leibniz Institute for Evolution and Biodiversity Science, Biodiversity Dynamics, Invalidenstr. 43, 10115 Berlin, Germany*

[26]*Across the River – a Transboundary Peace Park for Sierra Leone and Liberia, The Royal Society for the Protection of Birds, 164 Dama Road, Kenema, Sierra Leone*

[27]*Natural History Museum of Denmark, University of Copenhagen, Universitetsparken 15, 2100 Copenhagen, Denmark*

[28]*University of Cincinnati, Department of Biological Sciences, 614 Rieveschl Hall, Cincinnati OH 45220, USA.*

[29]*Life Sciences, Field Museum of Natural History, 1400 S. Lake Shore Dr., Chicago IL, 60605 USA.*

[30]*Department of Biology and Burke Museum of Natural History and Culture, University of Washington, Seattle, Washington, USA*

[31]*Life Sciences Department, Natural History Museum, London SW7 5BD, UK.*

[32]*Trier University, Biogeography Department, Universitätsring 15, 54295 Trier, Germany*

[33]*CIBIO Research Centre in Biodiversity and Genetic Resources, InBIO, Universidade do Porto, Campus Agrario de Vairão, Rua Padre Armando Quintas, No. 7, 4485-661 Vairão, Vila do Conde, Portugal*

[34]*Tropical Biodiversity Section, Science Museum of Trento, Corso del lavoro e della Scienza 3, 38122 Trento, Italy*

[35]*Royal Belgian Institute of Natural Sciences, OD Taxonomy and Phylogeny, Rue Vautier 29, B-1000 Brussels, Belgium*

[36]*Forestry Research Institute of Ghana, P.O. Box 63, Fumesua, Kumasi, Ghana*

[37]*Muséum National d'Histoire Naturelle, Département Origines et Evolution, UMR 7205 ISYEB, 25 rue Cuvier, 75005 Paris, France*

[38]*Institut National de Recherche en Sciences Exactes et Naturelles, BP 2400 Brazzaville, République du Congo*

*Corresponding author: Daniel M. Portik; danielportik@email.arizona.edu

ABSTRACT

Theory predicts that sexually dimorphic traits under strong sexual selection, particularly those involved with intersexual signaling, can accelerate speciation and produce bursts of diversification. Sexual dichromatism (sexual dimorphism in color) is widely used as a proxy for sexual selection and is associated with rapid diversification in several animal groups, yet studies using phylogenetic comparative methods to explicitly test for an association between sexual dichromatism and diversification have produced conflicting results. Sexual dichromatism is rare in frogs, but it is both striking and prevalent in African reed frogs, a major component of the diverse frog radiation termed Afrobatrachia. In contrast to most other vertebrates, reed frogs display female-biased dichromatism in which females undergo color transformation, often resulting in more ornate coloration in females than in males. We produce a robust phylogeny of Afrobrachia to investigate the evolutionary origins of sexual dichromatism in this radiation and examine whether the presence of dichromatism is associated with increased rates of net

diversification. We find that sexual dichromatism evolved once within hyperoliids and was followed by numerous independent reversals to monochromatism. We detect significant diversification rate heterogeneity in Afrobatrachia and find that sexually dichromatic lineages have double the average net diversification rate of monochromatic lineages. By conducting trait simulations on our empirical phylogeny, we demonstrate our inference of trait-dependent diversification is robust. Although sexual dichromatism in hyperoliid frogs is linked to their rapid diversification and supports macroevolutionary predictions of speciation by sexual selection, the function of dichromatism in reed frogs remains unclear. We propose that reed frogs are a compelling system for studying the roles of natural and sexual selection on the evolution of sexual dichromatism across both micro- and macroevolutionary timescales.

KEYWORDS

Anura, Afrobatrachia, diversification, color evolution, macroevolution, sexual selection

INTRODUCTION

In *The Descent of Man and Selection in Relation to Sex*, Darwin (1871) observed that many closely related taxa differed primarily in secondary sexual characters and suggested that sexual selection plays a role in the diversification of species. The concept of speciation through sexual selection was later developed into a theory that links the coevolution of secondary sexual traits and mating preferences to premating reproductive isolation (Lande 1981, 1982; Kirkpatrick 1982; West-Eberhard 1983). This conceptual framework predicts that both the strength of sexual selection and the prevalence of sexually selected traits have a positive association with speciation rate (Lande 1981, 1982; West-Eberhard 1983; Barraclough et al. 1995). If divergence in secondary sexual characters and sexual selection are indeed major drivers of speciation, then clades exhibiting elaborate sexually dimorphic traits and/or elevated sexual selection should display higher species richness and increased diversification rates at macroevolutionary scales. Empirically, these predictions have mixed support across a range of sexually dimorphic traits that serve as proxies for sexual selection (reviewed in Kraaijeveld et al. 2011), indicating that macroevolutionary trends for traits involved with intersexual signaling and mate-choice may differ from those more strongly influenced by intrasexual or natural selection. For example, traits under ecological selection such as body size dimorphism have no consistent relationship with diversification (Kraaijeveld et al. 2011), whereas sexual dichromatism, a form of sexual dimorphism in which the sexes differ in color, often functions as a mate recognition signal and is associated with diversification in several taxonomic groups (Misof 2002; Stuart-Fox & Owens 2003; Alfaro et al. 2009; Kazancıo□lu et al. 2009; Wagner et al. 2012). Accordingly, sexual dichromatism has become a widely used proxy for studying the effects of sexual selection on speciation rate. However, phylogenetic comparative analyses explicitly testing for an association

between sexual dichromatism and diversification have produced conflicting results, even in well-studied groups such as birds (Barraclough et al. 1995; Owens et al. 1999; Morrow et al. 2003; Phillimore et al. 2006; Seddon et al. 2013; Huang & Rabosky 2014) where sexual dichromatism plays an important role in signaling and mate-choice (Price 2008). Differences in methodologies and the spatial, temporal, and taxonomic scales among studies may partially explain these contrasting results. In particular, recent studies have highlighted concerns about the ability to distinguish between trait-dependent and trait-independent diversification scenarios using phylogenetic comparative methods (Rabosky & Goldberg 2015; Beaulieu & O'Meara 2016). In a broader sense, however, this disparity among studies may reflect more nuanced or novel mechanisms underlying the evolution of sexual dichromatism such that it does not consistently fit the conceptual framework of speciation by sexual selection. For instance, the striking sexual dichromatism in *Eclectus* parrots results from intrasexual competition to attract mates and intersexual differences in exposure to visual predators (Heinsohn et al. 2005). Likewise, the dynamic sexual dichromatism in frogs that form large breeding aggregations may serve to identify other competing males rather than to attract mates (Sztatecsny et al. 2012; Kindermann & Hero 2016; Bell et al. 2017b). Consequently, investigating the evolution of secondary sexual characters like dichromatism across ecologically diverse taxonomic groups is essential if we aim to generalize about the function of sexually dimorphic traits and better understand the roles of natural and sexual selection in biological diversification.

Secondary sexual traits are diverse and prevalent among anurans (frogs and toads), and include sexual size dimorphism, structures for acoustic signaling, nuptial pads, spines, elongated fingers, glands, and sexual dichromatism (Duellman & Trueb 1986). Sexual size dimorphism is common and occurs in >90% of species (Shine 1979; Han & Fu 2013), and body size evolution

153 of the sexes is often attributed to fecundity for females and intrasexual competition, energetic
154 constraints, agility, and predation for males (Salthe & Duellman 1973; Wells 1977; Shine 1979;
155 Woolbright 1983; De Lisle & Rowe 2013; Han & Fu 2013; Nali et al. 2014). Male frogs of most
156 species produce acoustic or vibrational signals to attract females, and these signals are essential
157 for mate recognition and relaying social information (Ryan 1980; Gerhardt 1994; Gerhardt &
158 Huber 2002). Structures like spines and tusks, which are present in males of many species, are
159 used in male-male combat (e.g. McDiarmid 1975) whereas the diverse assortment of glands and
160 nuptial pads, which are widespread in male frogs, are likely involved in courtship and amplexus
161 (Duellman & Trueb 1986). In contrast to these widespread secondary sexual characters, anuran
162 sexual dichromatism is rare, occurring in only ~2% of frog species (Bell & Zamudio 2012; Bell
163 et al. 2017b). Behavioral studies in a handful of frog species indicate that these sexual color
164 differences may be subject to natural selection as well as inter- and intrasexual selection (Mann
165 & Cummings 2009; Sztatecsny et al. 2012). Sexual selection on coloration has historically been
166 dismissed in frogs with the assumption that communication is predominately acoustic (reviewed
167 in Starnberger et al. 2014); however, several studies document the importance of color signals in
168 courtship behavior and mate-choice, even in nocturnal species (Gomez et al. 2009; Gomez et al.
169 2010; Jacobs et al. 2016; Yovanovich et al. 2017; Akopyan et al. 2018). If sexual dichromatism
170 in frogs contributes to premating reproductive isolation, then sexually dichromatic clades may fit
171 the conceptual framework of speciation by sexual selection and display higher species richness
172 and increased diversification rates at macroevolutionary scales.

173 The Afrobatrachia frog radiation (Arthroleptidae, Brevicipitidae, Hemisotidae,
174 Hyperoliidae) includes over 400 species distributed across sub-Saharan Africa that reflect much
175 of the morphological, ecological and reproductive mode diversity present in anurans (Portik &

Blackburn 2016). Afrobatrachian frogs display many unusual secondary sexual characters including the hair-like skin structures of male Hairy Frogs (*Trichobatrachus*), an elongate third digit in males (up to 40% of body length in *Arthroleptis* and *Cardioglossa*), extreme body size dimorphism (*Leptopelis, Chrysobatrachus, Breviceps*), and prominent pectoral glands (*Leptopelis*) or gular glands on the male vocal sac (Hyperoliidae). Afrobatrachian frogs also have the highest incidence of sexual dichromatism among anurans, which is striking and prevalent in many hyperoliid reed frogs (*Hyperolius, Heterixalus*). In sexually dichromatic hyperoliids, the difference in coloration is female-biased: both sexes exhibit a consistent juvenile coloration upon metamorphosis (termed Phase J), but at the onset of maturity sex steroids trigger a color and/or color pattern change in females (Phase F) whereas males typically retain the juvenile color pattern (Fig. 1) (Schiøtz 1967; Richards 1982; Hayes 1997; Hayes & Menendez 1999). In many dichromatic reed frog species adult males can also display the Phase F coloration, but this generally occurs in lower frequency than the Phase J morph (Fig. 1) (Schiøtz 1967, 1999; Amiet 2012; Kouamé et al. 2015; Portik et al. 2016a). The function of the ontogenetic color shift in female reed frogs is poorly understood (Bell & Zamudio 2012), but it may be similar to female-biased sexual dichromatism in other vertebrates, which can result from a reversal in mating system in which females compete for males (Andersson 1994) or sexual niche partitioning in which males and females use different habitats (Shine 1989; Heinsohn et al. 2005). Alternatively, distinct female color patterns in reed frogs may play a role in courtship and mate recognition at breeding sites where upwards of eight hyperoliid species congregate in a single night (Drewes & Vindum 1994; Kouamé et al. 2013; Portik et al. 2018). The link between sexual dichromatism and rapid speciation across disparate animal clades (Misof 2002; Stuart-Fox & Owens 2003; Alfaro et al. 2009; Kazancıo□lu et al. 2009; Wagner et al. 2012) demonstrates that when sexual

dichromatism functions primarily as an intersexual signal under strong sexual selection, there are predictable outcomes on diversification rate. Therefore, as a first step towards understanding the potential function of dichromatism in hyperoliids, including the plausibility of intersexual signaling, we aim to assess whether this trait fits the predictions of speciation by sexual selection on a macroevolutionary scale.

In this study, we reconstruct the evolutionary history of sexual dichromatism within Afrobatrachia and investigate whether diversification rate shifts in this continental radiation are associated with dichromatism. We produce a well-resolved species tree of Hyperoliidae from genomic data and greatly increased taxonomic sampling relative to previous studies (Wieczorek et al. 2000; Veith et al. 2009; Portik & Blackburn 2016). To explore the evolution of sexual dichromatism within the broader phylogenetic and biogeographic context of African frogs, we incorporate all published sequence data of Afrobatrachia to produce a robust, time-calibrated phylogeny. Using methods that improve the accuracy of character state reconstructions by accounting for trait and diversification rate heterogeneity (King & Lee 2015; Beaulieu & O'Meara 2016), we test the hypothesis that sexual dichromatism evolved repeatedly within Afrobatrachia (Veith et al. 2009). Finally, we estimate net diversification rates from our time-calibrated phylogeny using the hidden state speciation and extinction framework (HiSSE; Beaulieu & O'Meara 2016) and examine if diversification rate shifts occur within Afrobatrachia and if so, whether they are associated with the occurrence of sexual dichromatism. Given recent concerns raised about the ability to distinguish between trait-dependent and trait-independent diversification scenarios (Rabosky & Goldberg 2015; Beaulieu & O'Meara 2016), we assess the performance of available state-dependent diversification methods with a trait simulation study conducted using our empirical phylogeny.

MATERIALS & METHODS

Species Tree Estimation of Family Hyperoliidae

Taxonomic sampling.— We included 254 hyperoliid samples in our sequence capture experiment with multiple representatives per species when possible. Although there are 230 currently recognized hyperoliid species (AmphibiaWeb, 2018), this family is in a state of taxonomic flux with recent studies recommending both the synonymy of species names and the splitting of species complexes (Rödel et al. 2002; Rödel et al. 2003; Wollenberg et al. 2007; Rödel et al. 2009; Rödel et al. 2010; Schick et al. 2010; Conradie et al. 2012; Dehling 2012; Channing et al. 2013; Conradie et al. 2013; Greenbaum et al. 2013; Liedtke et al. 2014; Loader et al. 2015; Portik et al. 2016a; Bell et al. 2017a; Conradie et al. 2018). We estimate that our sampling represents approximately 143 distinct hyperoliid lineages including 12 of 17 described hyperoliid genera. The five unsampled genera are either monotypic (*Arlequinus*, *Callixalus*, *Chrysobatrachus*, *Kassinula*) or species poor (*Alexteroon*, 3 spp.). Our sampling of the remaining genera is proportional to their recognized diversity and includes several known species complexes with lineages not reflected in the current taxonomy. We also sampled outgroup species from the following families: Arthroleptidae (7 spp), Brevicipitidae (1 sp), Hemisotidae (1 sp), and Microhylidae (1 sp). Museum and locality information for all specimens is provided in Table S1.

Sequence capture data and alignments.— The full details of transcriptome sequencing, probe design, library preparation, sequence captures, and bioinformatics pipelines are described in Portik et al. (2016b), but here we outline major steps of the transcriptome-based exon captures.

We sequenced, assembled, and filtered the transcriptomes of four divergent hyperoliid species and selected 1,260 orthologous transcripts for probe design. We chose transcripts 500–850 bp in length that ranged from 5–15% average pairwise divergence. Five additional nuclear loci (*POMC*, *RAG-1*, *TYR*, *FICD* and *KIAA2013*) were also incorporated based on published sequence data (Portik & Blackburn 2016). The final marker set for probe design included 1,265 genes from four species and 5060 individual sequences, with a total of 995,700 bp of target sequence. These sequences were used to design a MYbaits-3 custom bait library (MYcroarray, now Arbor Biosciences) consisting of 120 mer baits and a 2X tiling scheme (every 60 bp), which resulted in 60,179 unique baits. Transcriptomes, target sequences, and probe designs are available on Dryad (Portik et al. 2016c).

Genomic DNA was extracted using a high-salt extraction method (Aljanabi & Martinez 1997) and individual genomic libraries were prepared following Meyer & Kircher (2010) with modifications described in Portik et al. (2016b). Samples were pooled for capture reactions based on phylogenetic relatedness, and the combined postcapture libraries were sequenced on three lanes of an Illumina HiSeq2500 with 100 bp paired-end reads. Raw sequence data were cleaned following Singhal (2013) and Bi et al. (2012), and the cleaned reads of each sample were *de novo* assembled, filtered, and mapped as described in Portik et al. (2016b). The final filtered assemblies were aligned using MAFFT (Katoh et al. 2002, 2005; Katoh & Standley 2013) and trimmed using TRIMAL (Capella-Gutierrez et al. 2009). We enforced additional post-processing filters for alignments, including a minimum length of 90 bp and a maximum of 30% total missing data across an alignment, resulting in 1,047 exon alignments totaling 561,180 bp.

Species tree estimation.— We used the sequence capture data set to estimate a species tree for

Hyperoliidae using ASTRAL-III (Mirarab et al. 2014; Mirarab & Warnow 2015; Zhang et al. 2017), which uses unrooted gene trees to estimate the species tree. This method employs a quartet-based approach that is consistent under the multi-species coalescent process, and therefore appropriate for resolving gene tree discordance resulting from incomplete lineage sorting (Mirarab et al. 2014; Mirarab & Warnow 2015). This approach also allows for missing taxa in alignments, which were present in our sequence capture data and are problematic for other coalescent-based summary methods such as MP-EST (Liu et al. 2010). We kept samples with the most complete sequence data to collapse the alignments to a single representative per lineage and generated unrooted maximum likelihood (ML) gene trees with 200 bootstrap replicates for each locus using RAxML v8 (Stamatakis 2014) under the GTRCAT model. The set of 1,047 gene trees was used to infer a species tree with ASTRAL-III, and node support was assessed with 1) quartet support values, or local posterior probabilities computed from gene tree quartet frequencies, which also allows the calculation of branch lengths in coalescent units (Sayyari & Mirarab 2016), and 2) 200 replicates of multi-locus bootstrapping, where each of the 200 RAxML bootstrap trees per locus are used to infer a species tree and a greedy consensus tree is created from the 200 species trees to calculate percent support across nodes (Seo 2008).

Evolutionary Relationships of Afrobatrachian Frogs

DNA barcoding.— We obtained sequence data from the mitochondrial marker 16S ribosomal RNA (*16S*) for all samples included in the sequence capture experiment and for additional species we were unable to include in our sequence capture experiment due to insufficient DNA yield. Polymerase chain reactions (PCRs) were carried out in 12.5 µl volumes consisting of: 1.25 µl Roche 10x (500 mM Tris/HCl, 100 mM KCl, 50 mM $(NH_4)_2$ SO_4, 20 mM $MgCl_2$,

pH = 8.3), 0.75 µl 25 mM $MgCl_2$, 0.75 µl 2 mM dNTPs, 0.25 µl 10.0 µM forward primer, 0.25 µl 10.0 µM reverse primer, 8.40 µl H_2O, 0.10 µl Taq, and 0.75 µl DNA. Amplification involved initial denaturation at 94°C for 4 min, followed by 35 cycles of 95°C for 60 s, 51°C for 60 s, 72°C for 90 s, and a final extension at 72°C for 7 min, using the primer pairs 16SA and 16SB (Palumbi et al. 1991). The PCR amplifications were visualized on an agarose gel, cleaned using ExoSAP-IT, and sequenced using BigDye v3.1 on an ABI3730 sequencer (Applied Biosystems). Newly generated sequences are deposited in GenBank (Accession numbers: XXXXX).

GenBank data.— To expand our taxonomic sampling we included all available published sequence data of Afrobatrachian frogs. We built a molecular data matrix using the five nuclear loci included in our captures (*FICD, KIAA2013, POMC, TYR,* and *RAG-1*) and the mtDNA marker *16S*. This resulted in the inclusion of 30 additional hyperoliids and 130 arthroleptid, brevicipitid, and hemisotid species, though many are represented solely by *16S* mtDNA data. Nuclear loci were aligned using MUSCLE (Edgar 2004), and *16S* sequences were aligned using MAFFT with the E-INS-i strategy (Katoh et al. 2002; Katoh et al. 2005). The final concatenated alignment of the expanded taxonomic data set consisted of 283 taxa and 3,991 bp, with 36% total missing data.

Phylogenetic methods and divergence dating analyses.— We reconstructed the phylogenetic relationships of Afrobatrachian frogs from the five nuclear gene and mtDNA data set using a maximum likelihood (ML) approach in RAXML v8 (Stamatakis 2014). To preserve the relationships inferred with our species tree analyses of sequence capture loci, the sequence capture hyperoliid species tree containing 153 taxa (143 ingroup and 10 outgroup taxa) was used

as a partial constraint tree for the ML analysis of the 283-taxon alignment of six loci. A preliminary step for our divergence dating analyses in BEAST v1.8.1 (Drummond et al. 2012) involved transforming the ML Afrobatrachian frog tree to an ultrametric tree, and for this we used penalized likelihood with the 'chronopl' function of APE (Sanderson 2002; Paradis et al. 2004), setting age bounds to allow divergence times to be compatible with our BEAST calibration priors. We performed analyses using a fixed ultrametric starting tree topology by removing relevant operators acting on the tree model. We used four secondary calibration points with normal distributions to constrain the most recent common ancestors (MRCAs) of Afrobatrachia to 80 Ma ± 5 SD, (Hemisotidae + Brevicipitidae) to 50 Ma ± 5 SD, Arthroleptidae to 40 Ma ± 5 SD, and Hyperoliidae to 40 Ma ± 5 SD, based on published age estimates of Afrobatrachian frogs (Roelants et al. 2007; Kurabayashi & Masayuki 2013; Loader et al. 2014; Portik & Blackburn 2016). We used the Yule model of speciation as the tree prior, applied an uncorrelated relaxed lognormal clock, and ran two analyses for 30,000,000 generations sampling every 3,000 generations. Runs were assessed using TRACER v1.5.0 (Rambaut et al. 2013) to examine convergence, and a maximum clade credibility tree with median heights was created from 7,500 trees after discarding a burn-in of 2,500 trees.

Evolution of Sexual Dichromatism and State-Dependent Diversification

We scored the presence or absence of sexual dichromatism for hyperoliid species in our data set from multiple sources, including publications (Schiøtz 1967, 1999; Channing 2001; Channing & Howell 2006; Wollenberg et al. 2007; Rödel et al. 2009; Veith et al. 2009; Amiet 2012; Bell & Zamudio 2012; Channing et al. 2013; Conradie et al. 2013; Portik et al. 2016a), examination of museum specimens (Portik 2015), and the collective field observations from all authors. A

337 species was considered sexually dichromatic if adult females and adult males exhibit distinct
338 color patterns (Phase F and Phase J, respectively), which also includes species with variation in
339 male color phase (males display Phase J and Phase F). A summary of the sexual dichromatism
340 data is provided in Table S2.

341 We reconstructed the evolution of sexual dichromatism on the time-calibrated phylogeny
342 of Afrobatrachia using Bayesian ancestral state reconstruction in BEAST (Drummond et al. 2012),
343 and also with hidden state speciation and extinction analyses using the R package HISSE
344 (Beaulieu & O'Meara 2016) (described below). We performed Bayesian ancestral state
345 reconstructions using several combinations of clock and character models in BEAST v1.8.1
346 (Drummond et al. 2012) following King and Lee (2015). The topology and branch lengths were
347 fixed by removing all tree operators, and sexual dichromatism was treated as a binary alignment.
348 Because all outgroup families are monochromatic, we fixed the root state by adding a
349 placeholder monochromatic taxon to the root with a zero branch length, creating a hard prior
350 distribution on the root where P(monochromatic root) = 1, and P(dichromatic root) = 0. A
351 stochastic Mk model of character evolution (Lewis 2001) was used with symmetrical (Mk1) or
352 asymmetrical (Mk2) transition rates between states, and each character model was analyzed
353 using a strict clock model (enforcing a homogenous trait rate) and a random local clock model
354 (allowing for heterotachy), resulting in four analysis combinations. The analyses involving the
355 random local clock allowed estimation of the number and magnitude of rate changes using
356 MCMC. All analyses were run for 200 million generations with sampling every 20,000
357 generations, resulting in 10,000 retained samples. We used the marginal likelihood estimator
358 with stepping stone sampling, with a chain length of 1 million and 24 path steps, to estimate the
359 log marginal likelihood of each run (Baele et al. 2012, 2013). We performed five replicates per

analysis to ensure consistency in the estimated log marginal likelihood, and subsequently compared the four different analyses using log Bayes factors, calculated as the difference in log marginal likelihoods, to select the best fit clock model and character model combination. We summarized transitions between character states and created consensus trees to estimate the posterior probabilities of a character states across nodes.

We performed hidden state speciation and extinction (HiSSE) analyses using the R package HISSE (Beaulieu & O'Meara 2016) to identify if sexual dichromatism in Afrobatrachian frogs is associated with increased diversification rates, and to reconstruct ancestral states while accounting for transition rate and diversification rate heterogeneity. The HiSSE model builds upon the popular binary-state speciation and extinction (BiSSE) model (Maddison et al. 2007) by incorporating 'hidden states' representing unmeasured traits that could impact the diversification rates estimated for states of the observed trait. The HiSSE model is therefore able to account for diversification rate heterogeneity that is not linked to the observed trait, while still identifying trait-dependent processes. The HiSSE framework also includes a set of null models that explicitly assume the diversification process is independent from the observed trait, without constraining diversification rates to be homogenous across the tree. The inclusion of these character-independent models circumvents a significant problem identified in the BiSSE framework, in which the simple 'null' model of constant diversification rates is typically rejected in favor of trait-dependent diversification when diversification rate shifts unrelated to the trait occur in the phylogeny (Rabosky & Goldberg 2015; Beaulieu & O'Meara 2016). The improved character-independent diversification models, referred to as CID-2 and CID-4, contain the same number of diversification rate parameters as the BiSSE and HiSSE models, respectively. We fit 26 different models to our sexual dichromatism data set (Table 1): six represent BiSSE-like

models, four are variations of the CID-2 model, five are variations of the CID-4 model, nine are various HiSSE models with two hidden states, and two are HiSSE models with a single hidden state. Within each of these classes, the models vary mainly in the number of distinct transition rates (q), extinction fraction rates (ε), and net turnover rates (τ), and the most complex HiSSE model includes four net turnover rates, four extinction fraction rates, and eight distinct transition rates. We enforced a monochromatic root state for all models and evaluated the fit of the 26 models using AIC scores, ΔAIC scores, and Akaike weights (ω_i) (Burnham & Anderson 2002). From the best-fit model, we estimated confidence intervals for relevant parameters and transformed ε and τ to obtain speciation (λ), extinction (μ), and net diversification rates using the 'SupportRegion' function in HISSE (Beaulieu & O'Meara 2016). We performed ancestral state estimations for each of the 26 models using the marginal reconstruction algorithm implemented in the 'MarginRecon' function of HISSE, again enforcing a monochromatic root state. Our final estimation and visualization of diversification rates and node character states on the Afrobatrachian phylogeny took model uncertainty into account by using the model averaging approach described by Beaulieu and O'Meara (2016), such that model contributions to rates and states were proportional to their likelihoods.

Simulated traits and state-dependent diversification.—The identified bias towards the detection of trait-dependent diversification in the BiSSE framework (Rabosky & Goldberg 2015; Beaulieu & O'Meara 2016) prompted us to investigate if a similar outcome would be detected in our data set, and whether the HiSSE framework could improve our ability to distinguish whether the observed states are correlated with diversification rates. One concern raised by Beaulieu and O'Meara (2016) is that neutrally evolving traits simulated on trees generated from a complex

406 heterogenous rate branching process can lead to false signals of trait-dependent diversification,
407 signifying the HiSSE framework may be sensitive to particular types of tree shapes.
408 To evaluate the performance of these methods given our empirical tree topology, we
409 simulated neutrally evolving traits on the Afrobatrachian frog phylogeny and tested for trait-
410 dependent diversification using both the BiSSE and HiSSE frameworks. We conducted
411 independent simulations of a binary trait with the 'sim.history' function in R package PHYTOOLS
412 (Revell 2012), using the unequal rates *q*-matrices obtained from our empirical data, enforcing a
413 root state of trait absence. We required a minimum of 10% of taxa to exhibit the derived state
414 and conducted simulations until we obtained 1,500 replicates meeting this criterion. We used
415 maximum likelihood to fit a BiSSE model and the typical 'null' model with equal speciation and
416 extinction rates to each simulated trait using the R package DIVERSITREE (Maddison et al. 2007;
417 FitzJohn et al. 2009; FitzJohn 2012). We performed likelihood ratio tests and calculated ΔAIC
418 scores to determine if the constraint model could be rejected with confidence (ΔAIC > 2 or p-
419 value < 0.05), and summarized the number of instances each of the two models was favored
420 across the simulations. We analyzed the simulated data in the HiSSE framework as with our
421 empirical data, but with a reduced set of five models representing each major category of model.
422 This reduced model set included two BiSSE-like models that differed only in the constraint of τ,
423 a CID-2 and CID-4 model, and a HiSSE model with two hidden states, three transition rates,
424 equal τ, and distinct τ. We set a probability of one for trait absence at the root state to match the
425 manner in which traits were simulated and evaluated the fit of the 5 models using ΔAIC scores
426 and Akaike weights (ω_i) for each simulation, using a threshold of ΔAIC greater than two to favor
427 a model. Specifically, we were interested in whether the unconstrained BiSSE-like or HiSSE
428 models were favored, resulting in the detection of a false pattern of trait-dependent

diversification, or if the CID-2 or CID-4 models were selected, capturing the expected pattern where the diversification process was independent from trait evolution.

RESULTS

Phylogenetic Relationships

The sequence capture data set consisting of 1,047 loci and 561,180 bp produced a well-resolved species tree with a normalized quartet score of 0.877 and only eight of 150 nodes (5%) with quartet scores below 0.9 (Fig. S1). The multilocus bootstrapping analysis produced similar results with low support for only seven nodes, six of which also received low support in the species tree analyses (Fig. S1). The higher-level relationships recovered in the species tree are largely congruent with those recovered by Portik and Blackburn (2016), though we found strong support for a different placement of the genus *Acanthixalus* as sister to the clade containing *Semnodactylus*, *Paracassina*, *Phlyctimantis*, and *Kassina*, which together are sister to all other hyperoliids. Our improved sampling provides the first comprehensive assessment of evolutionary relationships within the speciose genera *Afrixalus* and *Hyperolius*. The monophyly of *Hyperolius* is supported, however *Afrixalus* is paraphyletic, and we found a sister relationship between the Ethiopian-endemic *A. enseticola* and the Malagasy-Seychelles species of *Heterixalus* and *Tachycnemis*, which are in turn sister to all remaining *Afrixalus* (Fig. S1). We found strong support for the southern African species *Hyperolius semidiscus* as sister to all other lineages in the genus, and furthermore recovered *H. parkeri*, *H. lupiroensis* and the *H. nasutus* complex as sister to two larger subclades of *Hyperolius* (Clades 1 and 2; Figs. 2, S1). In an effort to distinguish the main division within Hyperoliidae, we recognize the subfamilies Kassininae Laurent, 1972 and Hyperoliinae Laurent, 1943 and define the content within each on the basis of

our species tree analysis as follows: 1) Kassininae: *Acanthixalus, Kassina, Paracassina, Phlyctimantis,* and *Semnodactylus,* 2) Hyperoliinae: *Afrixalus, Cryptothylax, Heterixalus, Hyperolius, Morerella,* and *Opisthothylax* (Fig. 2). We retain previous subfamily assignments for genera not sampled in our molecular study (Hyperoliinae: *Alexteroon*, *Arlequinus, Callixalus, Chrysobatrachus*, *Kassinula*), which should be included in future phylogenetic studies to confirm these placements.

The phylogenetic analyses of the Afrobatrachia supermatrix produced family-level relationships consistent with previous analyses (Pyron & Wiens 2011; Portik & Blackburn 2016; Feng et al. 2017), including a sister relationship between Hyperoliidae and Arthroleptidae, and between Hemisotidae and Brevicipitidae (Fig. S2). This expanded taxonomic data set also included improved sampling for the Malagasy hyperoliid genus *Heterixalus* and the *Hyperolius nasutus* complex, for which we recovered results consistent with Wollenberg et al. (2007) and Channing et al. (2013), respectively. We recovered an Eocene age for the time to most recent common ancestor (TMRCA) of the families Hyperoliidae, Arthroleptidae and Brevicipitidae, of approximately 42.4 Ma (95% HPD: 39.1–51.6 Ma), 45.4 Ma (95% HPD: 35.5–48.7 Ma), and 41.8 Ma (95% HPD: 33.9–49.8 Ma) (Fig. S2). These dates are younger than previous estimates (Roelants et al. 2007; Loader et al. 2014) but are consistent with more recent multilocus analyses (Portik & Blackburn 2016; Feng et al. 2017). We found diversification events began within Hyperoliinae approximately 35.8 Ma (95% HPD: 30.1–41.6 Ma) and within Kassininae approximately 38.3 Ma (95% HPD: 30.9–45.6 Ma). The majority of speciation events within *Hyperolius* occurred from the late Miocene to the Plio-Pleistocene (Fig. S2).

Evolution of Sexual Dichromatism and State-Dependent Diversification

We found sexual dichromatism occurs in 60 of the 173 (34%) hyperoliid frog species included in our analyses. The Bayesian ancestral state reconstructions using four model combinations produced different patterns of character reconstructions and rates of trait evolution (Fig. S3). Overall, we found models with asymmetric character transition rates (Mk2) outperformed those with symmetric rates (Mk1), regardless of the clock model used (log-transformed Bayes factor range: 3.40–10.39; Table 2). The analysis with the highest log-marginal likelihood incorporated the relaxed local clock (RLC) Mk2 model, though it was not a significantly better fit than the simpler strict clock (SC) Mk2 model (log-transformed Bayes factor of 0.10) indicating low variation in lineage-specific evolutionary rates for this trait. The ancestral character reconstructions of the SC Mk2 indicated a median of two transitions from monochromatism to dichromatism. However, the character reconstructions revealed that this estimate is due to low posterior probability estimates for two critical nodes within Hyperoliinae (Fig. S3), and the presence of dichromatism at either one or both of these nodes would result in a single origin of sexual dichromatism. By contrast, the SC Mk2 model demonstrated approximately 27 independent losses of sexual dichromatism within hyperoliids, including losses in entire groups (*Afrixalus*, *H. nasutus* complex) and numerous reversals within *Heterixalus* and *Hyperolius* (notably in Clade 2) (Fig. S4).

Our hidden state speciation and extinction analyses revealed that a HiSSE model with four net turnover rates, equal extinction fraction rates, and three distinct transition rates was the best-fit model (Model 19, Table 1). The second and third ranked models (ΔAIC of 1.0, 2.5) were also HiSSE models that varied in the number of extinction fraction rates or the number of transition rates. Together these three HiSSE models accounted for 84.1% of the model weight (Table 1) and support a signal of state-dependent diversification in which sexual dichromatism

498 and a hidden state are associated with diversification rates. The net diversification rates inferred
499 using the best-fit model were nearly twice as high in sexually dichromatic lineages (0.157) as
500 compared to monochromatic lineages (0.091) in the absence of the hidden state (Fig. 3), and the
501 combination of the hidden state and dichromatism or monochromatism resulted in much lower
502 net diversification rate estimates (0.02 and <0.001, respectively). The trait reconstructions for all
503 four state combinations indicated that the dichromatism plus hidden state combination was only
504 present in the MRCA of two genera (*Cryptothylax*, *Morerella*) (Fig. S5), and was associated with
505 a markedly lower diversification rate (Fig. 3). The model-averaged ancestral state
506 reconstructions demonstrated strong support for a single origin of sexual dichromatism and 25
507 independent reversals to monochromatism within Hyperoliinae, with reversal patterns similar to
508 the Mk2 analyses (Figs. 2, S5).
509
510 *Simulated traits and state-dependent diversification*.—Analyzed in the BiSSE framework, we
511 found that many of the trait simulations on the phylogeny of Afrobatrachia resulted in the
512 rejection of the 'null' model of equal diversification rates across character states. Based on the
513 significance of likelihood ratio tests, we rejected the 'null' model in favor of trait-dependent
514 diversification for 565 (37.6%) of our 1500 comparisons. We recovered similar results using a
515 delta AIC cutoff value of two, for which we found support for trait-dependent diversification in
516 546 (36.4%) of the simulations (Fig. 4). In many of these cases we found unexpectedly strong
517 support for the BiSSE model, and 160 (10.6%) of the comparisons resulted in delta AIC values
518 ranging from 10–40.
519 In contrast to the BiSSE analyses, the addition of the character independent models (CID-
520 2 and CID-4) in HiSSE dramatically reduced the detection of a false association between

simulated traits and diversification rates by providing appropriate null models. In addition to these two CID models, our set of five models also included two BiSSE-like models and a typical HiSSE model. Based on a delta AIC cutoff value of two, out of the 1500 analyses performed the CID-4 model was selected 1,132 times (75.4%), the HiSSE model was chosen 125 times (8.3%), and the remaining 243 analyses (16.2%) showed equivocal support (ΔAIC = 0–2) for either the CID-4 or HiSSE model (Fig. 5). In the cases of equivocal support, the CID-4 and HiSSE models were always the top two models, which should be interpreted as a lack of support for trait-dependent diversification. Our error rate with the HiSSE model being favored in only 8.3% of our simulations was substantially lower than the Beaulieu and O'Meara (2016) 'difficult tree' scenario in which the HiSSE model was favored in 29% of the data sets. These simulation results strongly suggest the branching pattern of our empirical phylogeny is not inherently problematic for the investigation of trait-dependent diversification using these available methods, adding support to our empirical analyses in which we detected an association between diversification rates and sexual dichromatism.

DISCUSSION

Hyperoliid Relationships and the Origin of Sexual Dichromatism

Afrobatrachian frogs account for more than half of all African amphibians and this continental radiation exhibits incredible variation in ecomorphology, reproductive mode, and other life history traits (Portik & Blackburn 2016). Within Afrobatrachia, the family Hyperoliidae is the most species-rich (~230 species) with surprisingly little diversity in ecomorphology and reproductive mode (Schiøtz 1967, 1999; Portik & Blackburn 2016), but with incredible variation in coloration and sexual dichromatism. These phenotypic characteristics have generated

544 considerable taxonomic confusion within hyperoliids (e.g. Ahl 1931), hindering a clear
545 understanding of species diversity and the evolutionary history of this radiation. Here, we have
546 produced the most comprehensive hyperoliid species tree to date and found support for an
547 Eocene origin of two subfamilies representing a major division withiin Hyperoliidae: Kassininae
548 (26 species) and Hyperoliinae (~200 species). Within Hyperoliinae, we clarified relationships
549 within the hyperdiverse genus *Hyperolius* (~150 species), which largely consists of two clades
550 (Figs. 2, S1, S2). These clades represent parallel rapid radiations with species distributed across a
551 variety of habitats and altitudes throughout sub-Saharan Africa, which showcases Hyperoliidae
552 as a rich comparative framework for future biogeographic research.

553 While both Kassininae and Hyperoliinae include colorful species, sexual dichromatism
554 only occurs within Hyperoliinae where it is present in the genera *Tachycnemis*, *Cryptothylax* and
555 *Morerella*, several species of *Heterixalus*, and more than half of the *Hyperolius* species we
556 sampled (Fig. 2, Table S2). A previous study hypothesized that sexual dichromatism evolved
557 multiple times within Hyperoliidae (Veith et al. 2009); however, we found overwhelming
558 support for a single origin of sexual dichromatism (Figs. 2, S3) and over twenty independent
559 reversals to monochromatism that range from early transitions that characterize entire genera
560 (e.g., *Afrixalus*) to recent reversals within *Heterixalus* and *Hyperolius* (Figs. 2, S4). This
561 transition bias from dichromatism to monochromatism also occurs in birds (Price & Birch 1996;
562 Omland 1997; Burns 1998; Kimball et al. 2001; Hofmann et al. 2008; Dunn et al. 2015; Schultz
563 & Burns 2017), in which secondary monochromatism can evolve as the result of a color change
564 in either sex (Kimball & Ligon 1999; Johnson et al. 2013; Price & Eaton 2014; Dunn et al. 2015;
565 Schultz et al. 2017). Similar transitional pathways to secondary monochromatism occur in
566 hyperoliids, in which females may lose the ability for color transformation at sexual maturity

(both sexes retain the Phase J juvenile coloration) or males undergo obligatory ontogenetic color change at maturity (both sexes develop Phase F coloration) (Figs. 1, 5). Characterizing juvenile coloration across species, which is undocumented in many hyperoliids, and documenting ontogenetic color change, including the prevalence of male color phases (Portik et al. 2016a), will be essential steps toward differentiating between these two forms of monochromatism. In experimental settings, the hormone estradiol induces color transformation in both sexes in the dichromatic species *H. argus* and *H. viridiflavus*, yet the effects of testosterone differ across species (Richards 1982; Hayes & Menendez 1999) suggesting that evolutionary transitions from dichromatism to monochromatism result directly from differences in hormone sensitivities among species. Reversals to monochromatism are especially prominent in *Hyperolius* Clade 2 (twelve independent events; Figs. 2, S4), highlighting the potential for future research in this group to identify the physiological basis and molecular underpinnings of these transitions. For example, three monochromatic species of the *H. cinnamomeoventris* complex that are endemic to the islands of São Tomé and Príncipe (*H. drewesi, H. molleri, H. thomensis*; both sexes with Phase F coloration) are derived from a mainland clade with sexually dichromatic (*H. cinnamomeoventris, H. olivaceus*; females Phase F, males Phase J) and monochromatic species (*H. veithi;* both sexes Phase J) (Fig. 5). Variation among these closely related species is well suited for investigating both the evolutionary and ecological contexts underlying transitions from sexual dichromatism to monochromatism.

Sexual Dichromatism is Linked to Increased Diversification Rates

Sexual dichromatism is an important predictor of diversification in several taxonomic groups including cichlids (Wagner et al. 2012), labrid fish (Alfaro et al. 2009; Kazancıo□lu et al. 2009),

590 agamid lizards (Stuart-Fox & Owens 2003), and dragonflies (Misof 2002); yet in birds, the
591 relationship between dichromatism and species richness/speciation rate varies among studies that
592 differ in methodology and evolutionary scale (Barraclough et al. 1995; Owens et al. 1999;
593 Morrow et al. 2003; Phillimore et al. 2006; Seddon et al. 2013; Huang & Rabosky 2014).
594 Though some state-dependent speciation and extinction model sets, such as the BiSSE method,
595 are no longer considered adequate for robustly detecting trait-dependent diversification (Rabosky
596 & Goldberg 2015; Beaulieu & O'Meara 2016), the HiSSE method contains an expanded model
597 set that can link diversification rate heterogeneity to observed traits, hidden traits, or character
598 independent processes. In particular, the inclusion of appropriate null models (character-
599 independent models) reduces the inference of trait-dependent diversification when a phylogeny
600 contains diversification rate shifts unrelated to the focal trait (Beaulieu & O'Meara 2016). Our
601 trait simulation study recapitulated this result (Fig. 4) while also demonstrating that the
602 branching pattern of our afrobatrachian phylogeny is unlikely to drive false inferences of trait-
603 dependent diversification using HiSSE (e.g., the "worst-case" scenario of Beaulieu & O'Meara
604 2016). We found that sexually dichromatic hyperoliid lineages have nearly double the average
605 diversification rate of monochromatic lineages, and that these diversification rates are not
606 inflated by a hidden trait. Arboreal oviposition and an associated shift to breeding in pond
607 systems both evolved within hyperoliids and were previously suggested as potential factors
608 influencing diversification (Portik & Blackburn 2016). In our analyses these traits may have
609 represented hidden factors co-distributed with dichromatism; however, the shift to the sexual
610 dichromatism plus hidden state character combination occurred only once in the common
611 ancestor of two genera (*Cryptothylax*, *Morerella*; Fig. S5) and is actually associated with lower
612 diversification rates (Fig. 3), indicating that these additional traits had little impact on our

613 analyses. Together, our results demonstrate that diversification rate heterogeneity occurs within
614 Afrobatrachia and that the origin and persistence of sexual dichromatism in hyperoliid frogs is
615 linked to their rapid diversification across sub-Saharan Africa.
616
617 *How Does Sexual Dichromatism Influence Diversification Rate?*
618 Sexual dichromatism is a common proxy for sexual selection in macroevolutionary studies
619 (reviewed in Kraaijeveld et al. 2011), especially for testing the prediction that clades with
620 variation in secondary sexual characters under strong sexual selection exhibit higher
621 diversification rates and species richness (Lande 1981, 1982; West-Eberhard 1983; Barraclough
622 et al. 1995). While our trait-dependent diversification analyses strongly support a faster rate of
623 net diversification associated with sexual dichromatism, we currently lack behavioral and natural
624 history data in hyperoliids to establish whether sexual dichromatism is actually under strong
625 sexual selection. At more recent timescales, speciation by sexual selection can result in a group
626 of closely related species with high ecological similarity but differing almost exclusively in
627 signaling traits (West-Eberhard 1983; Dominey 1984; Panhuis et al. 2001; Turelli et al. 2001;
628 Andersson 2004; Mendelson & Shaw 2005; Ritchie 2007; Safran et al. 2013). Frogs are
629 generally opportunistic gape-limited predators (Duellman & Trueb 1986), and in hyperoliids
630 food partitioning is strongly dictated by body size (Luiselli et al. 2004). In one well-characterized
631 community site, the females of seven syntopic sexually dichromatic *Hyperolius* species display
632 minimal body size differences (Portik et al. 2018) but show exceptional divergence in color
633 (Portik et al. 2016a). Five of these species occur in the predominantly dichromatic *Hyperolius*
634 Clade 1, and within this clade there are typically striking interspecific color differences in
635 females, but not males, among species (Fig. 5). This pattern of interspecific variation in

636 secondary sexual characters in the absence of ecological divergence is consistent with the
637 predictions of speciation by sexual selection, and by inference, would imply that dichromatism in
638 hyperoliids – specifically female color – is an essential mate recognition signal (*sensu*
639 Mendelson & Shaw 2012). In frogs, male calls are well-established mate recognition signals that
640 can be under strong sexual selection (Ryan 1980; Gerhardt 1994), and these acoustic signals are
641 demonstrably important for hyperoliid frogs. Males form dense breeding aggregations and
642 choruses (Bishop et al. 1995), calls differ between closely-related species (Schiøtz 1967, 1999;
643 Gilbert & Bell 2018), and females prefer conspecific calls over calls of syntopic heterospecifics
644 (Telford & Passmore 1981). However, visual displays can also serve as important courtship
645 signals in frogs, typically in conjunction with acoustic signaling (Gomez et al. 2009; Gomez et
646 al. 2010; Starnberger et al. 2014; Jacobs et al. 2016; Yovanovich et al. 2017; Akopyan et al.
647 2018). Although most studies have documented female preference for male coloration, the recent
648 discovery of female displays during nocturnal phyllomedusine treefrog courtship highlights the
649 possibility of male mate-choice and intersexual selection of female coloration (Akopyan et al.
650 2018). The lack of heterospecific matings among dichromatic species at high-diversity breeding
651 sites (Portik et al. 2018) strongly suggests behavioral isolation may be linked to divergent mate
652 recognition signals, including male call (Telford & Passmore 1981), gular gland compounds
653 (Starnberger et al. 2013), or female coloration. Our knowledge of reproductive behavior in
654 hyperoliids is largely based on a single dichromatic species (*H. marmoratus*; Dyson & Passmore
655 1988; Telford & Dyson 1988; Dyson et al. 1992; Jennions et al. 1995), and as such there may be
656 an overlooked role for mutual mate-choice in hyperoliids, in which females locate males by call
657 and/or pheromones and males assess color patterns of approaching females.
658 Although it can be tempting to equate sexually dimorphic traits such as dichromatism

659 with sexual selection, several alternative mechanisms may also contribute to female-biased
660 dichromatism in hyperoliids. For instance, aposematism is a widespread anti-predator
661 mechanism in frogs that is typically accompanied by the presence of skin toxins (reviewed in
662 Toledo & Haddad 2009; Rojas 2017), commonly alkaloids (Daly 1995). Sex-specific differences
663 in chemical defense occur in some frogs (Saporito et al. 2010; Jeckel et al. 2015); however, both
664 males and females of four dichromatic hyperoliids lacked alkaloids in their skin (Portik et al.
665 2015) suggesting that either aposematism is an unlikely explanation for ornate coloration or that
666 hyperoliids have evolved novel compounds for chemical defense. Female-biased dichromatism
667 has also been tied to sex-role reversal in fishes and birds (Roede 1972; Oring 1982; Berglund et
668 al. 1986a, 1986b; Eens & Pinxten 2000), in which females compete more intensely than males
669 for access to mates. This mechanism seems unlikely for hyperoliids because males in both
670 monochromatic and dichromatic species form dense choruses and compete intensely to attract
671 females, often engaging in combat (Telford 1985; Backwell & Passmore 1990). Finally, sexual
672 niche partitioning (Selander 1966; Shine 1989) can result in sexual dichromatism when the sexes
673 use different microhabitats, and as a consequence are subject to different selective pressures and
674 predation regimes (Heinsohn et al. 2005; Bell & Zamudio 2012). During the breeding season,
675 male hyperoliids are exposed on calling sites and Hayes (1997) proposed that more cryptic male
676 coloration may reduce predation pressure, a hypothesis that is consistent with greater
677 observations of predation events on females of dichromatic species (Grafe 1997; Portik et al.
678 2018). Quantifying differences in predation rates between the sexes, between monochromatic
679 and dichromatic species, and between Phase F and Phase J males within dichromatic species
680 would address whether this aspect of natural selection is also shaping the evolution of sexual
681 dichromatism. Although these mechanisms and other differences in natural selection pressures

682 may influence the evolution of sexual dichromatism in hyperoliids, they are generally not
683 expected to elevate rates of reproductive isolation or drive diversification rate shifts comparable
684 to the effects of sexual selection. Therefore, we propose that hyperoliids are a compelling system
685 for disentangling the roles of sexual selection and natural selection in the evolution of sexual
686 dichromatism, and how these mechanisms have promoted diversification at both
687 microevolutionary and macroevolutionary timescales.
688
689
690 **ACKNOWLEDGEMENTS**
691 Laboratory work conducted by DMP was funded by a National Science Foundation DDIG
692 (DEB: 1311006), a National Science Foundation grant (DEB: 1202609) awarded to D.C.
693 Blackburn, an Ecological, Evolutionary, and Conservation Genomics Research Award presented
694 by the American Genetic Association, the Museum of Vertebrate Zoology, and by R.C. Bell and
695 J.A. McGuire. This work used the Vincent J. Coates Genomics Sequencing Laboratory at UC
696 Berkeley, supported by NIH S10 Instrumentation Grants S10RR029668 and S10RR027303.
697 We thank the following institutions for accessioning field collections and for facilitating loan
698 access: California Academy of Sciences, Cornell University Museum of Vertebrates, Institut
699 national de Recherche en Sciences Exactes et Naturelles, Museum für Naturkunde, Berlin,
700 Muséum National d'Histoire Naturelle, Museum of Comparative Zoology, Museum of
701 Vertebrate Zoology, National Museum, Prague, Natural History Museum, London, North
702 Carolina Museum of Natural Sciences, Port Elizabeth Museum, Senckenberg Natural History
703 Collections Dresden, South African Institute for Aquatic Biodiversity, South African National
704 Biodiversity Institute, The Field Museum, Trento Museum of Science, University of Texas at El

Paso Biodiversity Collections, and the Zoological Natural History Museum, Addis Ababa University. All authors express thanks to the many government agencies, ministries, and departments that issued research permits and provided the access necessary to conduct their individual field work in sub-Saharan Africa.

711 **LITERATURE CITED**

712 Ahl E (1931) *Amphibia, Anura III, Polypedatidae*. Das Tierreich 55: xvi + 477.

713 Akopyan M, Kaiser K, Vega A, Savant NG, Owen CY, Dudgeon SR, Robertson JM (2018)
714 Melodic males and flashy females: geographic variation in male and female reproductive
715 behavior in red-eyed treefrogs (*Agalychnis callidryas*). *Ethology* 124:54−64.

716 Alfaro ME, Brock CD, Banbury BL, Wainwright PC (2009) Does evolutionary innovation in
717 pharyngeal jaws lead to rapid lineage diversification in labrid fishes? *BMC Evol Biol* 9:255.

718 Aljanabi S, Martinez I (1997) Universal and rapid salt-extraction of high quality genomic DNA
719 for PCR-based techniques. *Nucleic Acids Res* 25:4692–4693.

720 Amiet J-L (2012) *Les Rainettes du Cameroun (Amphibiens Anoures)*. Saint-Nazaire, France: La
721 Nef des Livres. 591 pp.

722 AmphibiaWeb (2018) Available at: amphibiaweb.org. University of California, Berkeley.
723 Accessed May 2018.

724 Andersson M (1994) *Sexual selection*. Princeton, NJ. Princeton University Press.

725 Backwell PRY, Passmore NI (1990) Aggressive interactions and intermale spacing in choruses
726 of the leaf-folding frog, *Afrixalus delicatus*. *S Afr J Zool* 25:133–137.

727 Baele G, Lemey P, Bedford T, Rambaut A, Suchard MA, Alekseyenko AV (2012) Improving the
728 accuracy of demographic and molecular clock model comparison while accommodating
729 phylogenetic uncertainty. *Mol Biol Evol* 29:2157–2167.

730 Baele G, Li WLS, Drummond AJ, Suchard MA, Lemey P (2012) Accurate model selection of
731 relaxed molecular clocks in Bayesian phylogenetics. *Mol Biol Evol* 30:239–243.

732 Barraclough TG, Harvey PH, Nee S (1995) Sexual selection and taxonomic diversity in
733 passerine birds. *Proc R Soc Lon B* 259:211−215.

734 Beaulieu JM, O'Meara BC (2016) Detecting hidden diversification shifts in models of trait-
735 dependent speciation and extinction. *Syst Biol* 65:583−601.
736 Bell RC, Zamudio KR (2012) Sexual dichromatism in frog: natural selection, sexual selection
737 and unexpected diversity. *Proc R Soc Lon B* 279:4687−4693.
738 Bell RC, Parra JL, Badjedjea G, Barej MF, Blackburn DC, Burger M, Channing A, Dehling JM,
739 Greenbaum E, Gvoždík V, Kielgast J, Kusamba C, Lötters S, McLaughlin PJ, Nagy ZT,
740 Rödel M-O, Portik DM, Stuart BL, VanDerWal J, Zamudio KR (2017a) Idiosyncratic
741 responses to climate-driven forest fragmentation and marine incursions in reed frogs from
742 Central Africa and the Gulf of Guinea Islands. *Mol Ecol* 26:5223–5224.
743 Bell RC, Webster GN, Whiting MJ (2017b) Breeding biology and the evolution of dynamic
744 sexual dichromatism in frogs. *J. Evol. Biol*. 30:2104−2115.
745 Berglund A, Rosenqvist G, Svensson I (1986a) Reversed sex roles and parental energy
746 investment in zygotes of two pipefish (Syngnathidae) species. *Mar Ecol Prog Ser* 29:209–
747 215.
748 Berglund A, Rosenqvist G, Svensson I (1986b) Mate choice, fecundity and sexual dimorphism in
749 two pipefish species (Syngnathidae). *Behav Ecol Sociobiol* 19:301–307.
750 Bi K, Vanderpool D, Singhal S, Linderoth T, Moritz C, Good JM (2012) Transcriptome-based
751 exon capture enables highly cost-effective comparative genomic data collection at moderate
752 evolutionary scales. *BMC Genomics* 13:403.
753 Bishop PJ, Jennions MD, Passmore NI (1995) Chorus size and call intensity: female choice in
754 the painted reed frog, *Hyperolius marmoratus*. *Behaviour* 132:721–731.
755 Burnham KP, Anderson DR (2002) *Model Selection and Multimodel Inference: A Practical*
756 *Information-Theoretic Approach*. New York: Springer.

757 Burns K (1998) A phylogenetic perspective on the evolution of sexual dichromatism in tanagers
758 (Thraupidae): the role of female versus male plumage. *Evolution* 52:1219–1224.
759 Capella-Gutierrez S, Silla-Martinez JM, Gabaldon T (2009) trimAl: a tool for automated
760 alignment trimming in large-scale phylogenetic analyses. *Bioinformatics* 25:1972–1973.
761 Channing A (2001) *Amphibians of Central and Southern Africa*. Cornell University Press,
762 Ithaca, New York, USA.
763 Channing A, Howell KM (2006) *Amphibians of East Africa*. Edition Chimaira, Frankfurt,
764 Germany.
765 Channing A, Hillers A, Lötters S, Rödel M-O, Schick S, Conradie W, Rödder D, Mercurio V,
766 Wagner P, Dehling JM, du Preez LH, Kielgast J, Burger M (2013) Taxonomy of the super-
767 cryptic *Hyperolius nasutus* group of long reed frogs of Africa (Anura: Hyperoliidae), with
768 descriptions of six new species. *Zootaxa* 3620:301–350.
769 Conradie W, Branch WR, Measey GJ, Tolley KA (2012) A new species of *Hyperolius* Rapp,
770 1842 (Anura: Hyperoliidae) from the Serra da Chela mountains, south-western Angola.
771 *Zootaxa* 3269:1–17.
772 Conradie W, Branch WR, Tolley KA (2013) Fifty shades of grey: giving colour to the poorly
773 known Angolan Ashy reed frog (Hyperoliidae: *Hyperolius cinereus*), with the description of
774 a new species. *Zootaxa* 3635:201–223.
775 Conradie W, Verbugt L, Portik DM, Ohler A, Bwong BA, Lawson LP (2018) A new reed frog
776 (Hyperoliidae: *Hyperolius*) from coastal northeastern Mozambique. Zootaxa 4379:177−198.
777 Daly JW (1995) The chemistry of poisons in amphibian skin. *Chemical ecology: the chemistry of*
778 *biotic interaction*, eds Eisner T, Meinwald J (National Academy Press, Washington, DC,
779 USA), pp 17–28.

780 Darwin CR (1871) *The Descent of Man, and Selection in Relation to Sex*. London: John Murray.
781 Volume 1. 1st edition.
782 De Lisle, SP, Rowe L (2013) Correlated evolution of allometry and sexual dimorphism across
783 higher taxa. *Am Nat* 183:630–639.
784 Dehling JM (2012) An African glass frog: a new *Hyperolius* species (Anura: Hyperoliidae) from
785 Nyungwe National Park, southern Rwanda. *Zootaxa* 3391:52–64.
786 Dominey W (1984) Effects of sexual selection and life history on speciation: species flocks in
787 African cichlids and Hawaiian *Drosophila*. *Evolution of Fish Species Flocks*, eds Echelle
788 AA, Kornfield I (University of Maine Press, Orono), pp 231−249.
789 Drewes RC, Vindum JV (1994) Amphibians of the Impenetrable Forest, Southwest Uganda. *J*
790 *Afr Zool* 108:55–70.
791 Drummond AJ, Suchard MA, Xie D, Rambaut A (2012) Bayesian phylogenetics with BEAUti
792 and the BEAST 1.7. *Mol Biol Evol* 29:1969–1973.
793 Duellman WE, Trueb L (1986) *Biology of Amphibians*. McGraw-Hill. New York, USA.
794 Dunn PO, Armenta JK, Whittingham LA (2015) Natural and sexual selection act on different
795 axes of variation in avian plumage color. *Sci Adv* 1:e1400155.
796 Dyson ML, Passmore NI (1988) Two-choice phonotaxis in *Hyperolius marmoratus* (Anura:
797 Hyperoliidae): the effect of temporal variation in presented stimuli. *Anim Behav* 36:648–652.
798 Dyson ML, Passmore NI, Bishop PJ, Henzi SP (1992) Male behavior and correlates of mating
799 success in a natural population of African painted reed frogs (*Hyperolius marmoratus*).
800 *Herpetologica* 48:236–246.
801 Edgar RC (2004) MUSCLE: multiple sequence alignment with high accuracy and high
802 throughput. *Nucl Acids Res* 32:1792–1797.

803 Eens M, Pinxten R (2000) Sex-role reversal in vertebrates: behavioural and endocrinological
804 accounts. *Behav Process* 51:135−147.
805 Feng Y-J, Blacburn DC, Liang D, Hillis DM, Wake DB, Cannatella DC, Zhang P (2017)
806 Phylogenomics reveals rapid, simultaneous diversification of three major clades of
807 Gondwanan frogs at the Cretaceous-Paleogene boundary. *Proc Natl Acad Sci USA*
808 114:E5864−E5870.
809 FitzJohn RG (2012) Diversitree: comparative phylogenetic analyses of diversification in R.
810 *Methods Ecol Evol* 3:1084–1092.
811 FitzJohn RG, Maddison WP, and Otto SP (2009) Estimating trait-dependent speciation and
812 extinction rates from incompletely resolved phylogenies. *Syst Biol* 58:595−611.
813 Gerhardt HC (1994) The evolution of vocalization in frogs and toads. *Annu Rev Ecol Syst*
814 25:233−324.
815 Gerhardt HC, Huber F (2002) *Acoustic communication in insects and anurans: common*
816 *problems and diverse solutions*. Chicago (IL): The University of Chicago Press.
817 Gilbert CM, Bell RC (2018) Evolution of advertisement calls in an island radiation of African
818 reed frogs. *Biol J Linn Soc* 123:1−11.
819 Gomez D, Richardson C, Lengagne T, Plenet S, Joly P, Léna J-P, Théry M (2009) The role of
820 nocturnal vision in mate choice: females prefer conspicuous males in the European tree frog
821 (*Hyla arborea*). *Proc R Soc B* 276:2351−2358.
822 Gomez D, Richardson C, Lengagne T, Derex M, Plenet S, Joly P, Léna J-P, Théry M (2010)
823 Support for a role of colour vision in mate choice in the nocturnal European treefrog.
824 *Behaviour* 147:1753−1768.
825 Grafe TU (1997) Costs and benefits of mate choice in the lek-breeding reed frog, *Hyperolius*

826 *marmoratus*. *Anim Behav* 53:1103–1117.

827 Greenbaum E, Sinsch U, Lehr E, Valdez F, Kusamba C (2013) Phylogeography of the reed frog
828 *Hyperolius castaneus* (Anura: Hyperoliidae) from the Albertine Rift of Central Africa:
829 implications for taxonomy, biogeography and conservation. *Zootaxa* 3131:473–494.

830 Han X, Fu J (2013) Does life history shape sexual size dimorphism in anurans? A comparative
831 analysis. *BMC Evol Biol* 13:27.

832 Hayes TB (1997) Hormonal mechanisms as potential constraints on evolution: examples from
833 the Anura. *Am Zool* 37:482−490.

834 Hayes TB, Menendez KP (1999) The effect of sex steroids on primary and secondary sex
835 differentiation in the sexually dichromatic reedfrog (*Hyperolius argus*: Hyperolidae) from the
836 Arabuko Sokoke forest of Kenya. *Gen Comp Endocr* 115:188−199.

837 Heinsohn R, Legge S, Endler JA (2005) Extreme reversed sexual dichromatism in a bird without
838 sex role reversal. *Science* 309:617−619.

839 Hofmann CM, Cronin TW, Omland KE (2008) Evolution of sexual dichromatism. 1. Convergent
840 losses of elaborate female coloration in New World orioles (*Icterus* spp.) *Auk* 125:778−789.

841 Huang H, Rabosky DL (2014) Sexual selection and diversification: reexamining the correlation
842 between dichromatism and speciation rate in birds. *Am Nat* 184(5):E104−E114.

843 Jacobs LE, Vega A, Dudgeon S, Kaiser K, Robertson JM (2016) Local not vocal: assortative
844 female choice in divergent populations of red-eyed treefrogs, *Agalychnis callidryas* (Hylidae:
845 Phyllomedusinae). *Biol J Linn Soc* 120:171−178.

846 Jeckel AM, Grant T, Saporito RA (2015) Sequestered and synthesized chemical defenses in the
847 poison frog *Melanophryniscus moreirae*. *J Chem Ecol* 41:505–512.

848 Jennions MD, Bishop PJ, Backwell PRY, Passmore NI (1995) Call rate variability and female

choice in the African frog, *Hyperolius marmoratus*. *Behaviour* 132:709–720.

Johnson AE, Price JJ, Pruett-Jones S (2013) Different modes of evolution in males and females generate dichromatism in fairy-wrens (Maluridae). *Ecol Evol* 3:3030–3046.

Kazancıo□lu E, Near TJ, Hanel R, Wainwright PC (2009) Influence of sexual selection and feeding functional morphology on diversification rate of parrotfishes. *Proc R Soc B* 276:3439−3446.

Katoh K, Standley DM (2013) MAFFT multiple sequence alignment software version 7: improvements in performance and usability. *Mol Biol Evol* 30:722–780.

Katoh K, Kuma K, Toh H, Miyata T (2005) MAFFT version 5: improvement in accuracy of multiple sequence alignment. *Nucleic Acids Res* 33:511–518.

Katoh K, Misawa K, Kuma K, Miyata T (2002) MAFFT: a novel method for rapid multiple sequence alignment based on fast Fourier transform. *Nucleic Acids Res* 30:3059–3066.

Kimball RT, Ligon JD (1999) Evolution of avian plumage dichromatism from a proximate perspective. *Am Nat* 154(2):182−193.

Kimball RT, Braun EL, Ligon JD, Lucchini V, Randi E (2001) A molecular phylogeny of the peacock-pheasants (Galliformes: *Polyplectron* spp.) indicates loss and reduction of ornamental traits and display behaviours. *Biol J Linn Soc* 73:187−198.

Kindermann C, Hero J-M (2016) Rapid dynamic colour change is an intrasexual signal in a lek breeding frog (*Litoria wilcoxii*). *Behav Ecol Sociobiol* 70:1995−2003.

King B, Lee MSY (2015) Ancestral state reconstruction, rate heterogeneity, and the evolution of reptile viviparity. *Syst Biol* 64:532−544.

Kirkpatrick M (1982) Sexual selection and the evolution of female choice. *Evolution* 36:1−12.

Kouamé N'GG, Boateng CO, Rödel M-O (2013) A rapid survey of the amphibians from the

872 Atewa Range Forest Reserve, Eastern Region, Ghana. *A Rapid Biological Assessment of the*
873 *Atewa Range Forest Reserve, Eastern Ghana*, ed. Conservation International (Arlington,
874 Virginia), pp 76–83.
875 Kouamé AM, Kouamé N'GG, Konan JCBYN'G, Adepo-Gourène B, Rödel M-O (2015)
876 Contributions to the reproductive biology and behaviour of the dotted reed frog, *Hyperolius*
877 *guttulatus*, in southern-central Ivory Coast, West Africa. *Herpetology Notes* 8:633−641.
878 Kraaijeveld K, Kraaijeveld-Smit FJL, Maan ME (2011) Sexual selection and speciation: the
879 comparative evidence revisited. *Biol Rev* 86:367−377.
880 Kurabayashi A, Sumida M (2013) Afrobatrachian mitochondrial genomes: genome
881 reorganization, gene rearrangement mechanisms, and evolutionary trends of duplicated and
882 rearranged genes. *BMC Genomics* 14:633.
883 Lande R (1981) Models of speciation by sexual selection on polygenic traits. *Proc Natl Acad Sci*
884 *USA* 78:3721−3725.
885 Lande R (1982) Rapid origin of sexual isolation and character displacement in a cline. *Evolution*
886 36:213−223.
887 Lewis PO (2001) A likelihood approach to estimating phylogeny from discrete morphological
888 character data. *Syst Biol* 50:913–925.
889 Liedtke HC, Hügil D, Dehling JM, Pupin F, Menegon M, Plumptre AJ, Kujirakwinja D, Loader
890 SP (2014) One or two species? On the case of *Hyperolius discodactylus* Ahl, 1931 and *H.*
891 *alticola* Ahl, 1931 (Anura: Hyperoliidae). *Zootaxa* 3768:253–290.
892 Liu L, Yu L, Edwards SV (2010) A maximum pseudo-likelihood approach for estimating species
893 trees under the coalescent model. *BMC Evol Biol* 10:302.
894 Loader SP, Ceccarelli FS, Menegon M, Howell KM, Kassahun R, Mengistu AA, Saber SA,

Gebresenbet F, de Sa R, Davenport TRB, Larson JG, Müller H, Wilkinson M, Gower DJ (2014) Persistence and stability of Eastern Afromontane forests: evidence from brevicipitid frogs. *J Biogeogr* 41:1781–1792.

Loader SP, Lawson LP, Portik DM, Menegon M (2015) Three new species of spiny throated reed frogs (Anura: Hyperoliidae) from evergreen forests of Tanzania. *BMC Research Notes* 8:167.

Luiselli L, Bikikoro L, Odegbune E, Wariboko SM, Rugiero L, Akani GC, Politano E (2004) Feeding relationships between sympatric Afrotropical frogs (genus *Hyperolius*): the effects of predator body size and season. *Animal Biology* 54:293−302.

Maddison WP, Midford PE, Otto SP (2007) Estimating a binary character's effect on speciation and extinction. *Syst Biol* 56:701−710.

Maan ME, Cummings ME (2009) Sexual dimorphism and directional sexual selection on aposematic signals in a poison frog. *Proc Natl Acad Sci USA* 106:19072–19077.

McDiarmid RW (1975) Glass frog romance along a tropical stream. *Nat. Hist. Mus. Los Angeles Co. Terra.* 13(4):14−18.

Mendelson TC, Shaw KL (2012) The (mis)concept of species recognition. *Trends Ecol. Evol.* 27:421−427.

Meyer M, Kircher M (2010) Illumina sequencing library preparation for highly multiplexed target capture and sequencing. *Cold Spring Harbor Protocols* 2010:pdb.prot5448.

Mirarab S, Warnow T (2015) ASTRAL-II: coalescent-based species tree estimation with many hundreds of taxa and thousands of genes. *Bioinformatics* 31:i44–i52.

Mirarab S, Reaz R, Bayzid MdS., Zimmermann T, Swenson MS, Warnow T (2014) ASTRAL: genome-scale coalescent-based species tree estimation. *Bioinformatics* 30:i541–i548.

Misof B (2002) Diversity of Anisoptera (Odonata): inferring speciation processes from patterns of morphological diversity. *Zoology* 105:355−365.

Morrow EH, Pitcher TE, Anrqvist G (2003) No evidence that sexual selection is an 'engine of speciation' in birds. *Ecol Lett* 6:228−234.

Nali RC, Zamudio KR, Haddad CFB, Prado CPA. 2014. Size-dependent selective mechanisms on males and females and the evolution of sexual size dimorphism in frogs. *Am Nat* 184:727–740.

Omland KE (1997) Examining two standard assumptions of ancestral reconstructions: repeated loss of dichromatism in dabbling ducks. *Evolution* 51:1636−1646.

Oring LW (1982) Avian mating systems. *Avian Biology*, eds Farner DS, King JS, Parkes KC (Academic Press, New York), pp 1–92.

Owens IPF, Bennett PM, Harvey PH (1999) Species richness among birds: body size, life history, sexual selection or ecology? *Proc R Soc Lon B* 266:933−939.

Palumbi S, Martin A, Romano S, McMillan WO, Stice L, Grabowski G (1991) *The Simple Fool's Guide to PCR. Version 2*. Honolulu: University of Hawaii.

Panhuis TM, Butlin R, Zuk M, Tregenza T (2001) Sexual selection and speciation. *Trends Ecol Evol* 16(7):364−371.

Paradis E, Claude J, Strimmer K (2004) APE: analysis of phylogenetics and evolution in R language. *Bioinformatics* 20:289–290.

Phillimore AB, Freckleton RP, Orme CDL, Owens IPF (2006) Ecology predicts large-scale patterns of phylogenetic diversification in birds. *Am Nat* 168(2):220−229.

Portik DM (2015) *Diversification of Afrobatrachian frogs and the herpetofauna of the Arabian Peninsula*. PhD Thesis. University of California, Berkeley.

941 Portik DM, Blackburn DC (2016) The evolution of reproductive diversity in Afrobatrachia: a
942 phylogenetic comparative analysis of an extensive radiation of African frogs. *Evolution*
943 70(9):2017−2032.
944 Portik DM, Scheinberg L, Blackburn DC, Saporito RA (2015) Lack of defensive alkaloids in the
945 integumentary tissue of four brilliantly colored African reed frog species (Hyperoliidae:
946 *Hyperolius*). *Herpetological Conservation and Biology* 10:833−838.
947 Portik DM, Jongsma GF, Kouete MT, Scheinberg LA, Freiermuth B, Tapondjou WP, Blackburn
948 DC (2016a) A survey of amphibians and reptiles in the foothills of Mount Kupe, Cameroon.
949 *Amphibian and Reptile Conservation* 10(2)[Special Section]:37–67(e131).
950 Portik DM, Smith LL, Bi K (2016b) An evaluation of transcriptome-based exon capture for frog
951 phylogenomics across multiple scales of divergence (Class: Amphibia, Order: Anura). *Mol*
952 *Ecol Resour* 16:1069–1083.
953 Portik DM, Smith LL, Bi K (2016c) Data from: An evaluation of transcriptome-based exon
954 capture for frog phylogenomics across multiple scales of divergence (Class: Amphibia,
955 Order: Anura). *Dryad Digital Repository*. https://doi.org/10.5061/dryad.pr3pr.
956 Portik DM, Jongsma GF, Kouete MT, Scheinberg LA, Freiermuth B, Tapondjou WP, Blackburn
957 DC (2018). Ecological, morphological, and reproductive aspects of a diverse assemblage of
958 hyperoliid frogs (Family: Hyperoliidae) surrounding Mt. Kupe, Cameroon. *Herpetol Rev*, In
959 Press.
960 Price JJ, Eaton MD (2014) Reconstructing the evolution of sexual dichromatism: current color
961 diversity does not reflect past rates of male and female change. *Evolution* 68:2026−2037.
962 Price T (1998) Sexual selection and natural selection in bird speciation. *Phil Trans R Soc Lond B*
963 353:251−260.

964 Price T, Birch GL (1996) Repeated evolution of sexual color dimorphism in passerine birds. *Auk*
965 113:842−848.
966 Pyron RA, Wiens JJ. 2011. A large-scale phylogeny of Amphibia including over 2800 species,
967 and a revised classification of extant frogs, salamanders, and caecilians. *Mol Phylogenet Evol*
968 61:543–583.
969 Rabosky DL, Goldberg EE (2015) Model inadequacy and mistaken inferences of trait-dependent
970 speciation. *Syst Biol* 64:340–355.
971 Rambaut A, Drummond AJ, Suchard M (2013). Tracer v1.6.0. Available from:
972 http://beast.bio.ed.ac.uk/
973 Revell LJ (2012) Phytools: an R package for phylogenetic comparative biology (and other
974 things). *Methods Ecol Evol* 3:217–223.
975 Richards CM (1982) The alteration of chromatophore expression by sex hormones in the Kenyan
976 Reed Frog, *Hyperolius viridiflavus*. *General and Comparative Endocrinology* 46:59−67.
977 Ritchie MG (2007) Sexual selection and speciation. *Ann Rev Ecol Evol S* 38:79−102.
978 Rödel M-O, Grafe TU, Rudolf VHW, Ernst R (2002) A review of West African spotted *Kassina*,
979 including a description of *Kassina schioetzi* sp. nov. (Amphibia: Anura: Hyperoliidae).
980 *Copeia* 2002:800–814.
981 Rödel M-O, Kosuch J, Veith M, Ernst R (2003) First record of the genus *Acanthixalus* Laurent,
982 1944 from the Upper Guinean Rain Forest, West Africa, with the description of a new
983 species. *J Herpetol* 37:43–52.
984 Rödel M-O, Kosuch J, Grafe TU, Boistel R, Assemian NE, Kouamé NG, Tohé B, Gourène G,
985 Perret J-L, Henle K, Tafforeau P, Pollet N, Veith M (2009) A new tree-frog genus and
986 species from Ivory Coast, West Africa (Amphibia: Anura: Hyperoliidae). *Zootaxa* 2044:23–

45.

Rödel M-O, Sandberger L, Penner J, Mané Y, Hillers A (2010) The taxonomic status of *Hyperolius spatzi* Ahl, 1931 and *Hyperolius nitidulus* Peters, 1875 (Amphibia: Anura: Hyperoliidae). *Bonn Zoological Bulletin* 57:177–188.

Roede M (1972) Color as related to size, sex and behavior in seven Caribbean labrid fish species (genera *Thalasoma, Halichoeres* and *Hemipteronotus*). *Studies on the fauna of Curacao and other Caribbean Islands* 42:1−266.

Roelants K, Gower DJ, Wilkinson M, Loader SP, Biju SD, Guillaume K, Moriau L, Bossuyt F (2007) Global patterns of diversification in the history of modern amphibians. *Proc Natl Acad Sci USA* 104:887–892.

Ryan MJ (1980) Female choice in a Neotropical frog. *Science* 209:523−525.

Safran RJ, Scordato ESC, Symes LB, Rodríguez RL, Mendelson TC (2013) Contributions of natural and sexual selection to the evolution of premating reproductive isolation: a research agenda. *Trends Ecol. Evol.* 28:643−650.

Salthe SN, Duellman WE (1973) Quantitative constraints associated with reproductive mode in anurans. *Evolutionary Biology of the Anurans*, ed Vial JL (University of Missouri Press, Missouri), pp 229–249.

Sanderson MJ (2002) Estimating absolute rates of molecular evolution and divergence times: a penalized likelihood approach. *Mol Biol Evol* 19:101–109.

Saporito RA, Donnelly MA, Spande TF, Garraffo HM (2012) A review of chemical ecology in poison frogs. *Chemoecology* 22:159–168.

Sayyari E, Mirarab S (2016) Fast coalescent-based computation of local branch support from quartet frequencies. *Mol Biol Evol* 33:1654–1668.

1010 Schick S, Kielgast J, Rödder D, Muchai V, Burger M, Lötters S (2010) New species of reed frog
1011 from the Congo Basin with discussion of paraphyly in cinnamon-belly reed frogs. *Zootaxa*
1012 2501:23–36.
1013 Schiøtz A (1967) The treefrogs (Rhacophoridae) of West Africa. *Spolia Zoologica Musei*
1014 *Hauniensis* 25:1−346.
1015 Schiøtz A (1999) *Treefrogs of Africa*. Edition Chimaira, Frankfurt, Germany.
1016 Seddon N, Botero CA, Tobias JA, Dunn PO, MacGregor HEA, Rubenstein DR, Uy AC, Weir
1017 JT, Whittingham LA, Safran RJ (2013) Sexual selection accelerates signal evolution during
1018 speciation in birds. *Proc R Soc B* 280:20131065.
1019 Selander RK (1966) Sexual dimorphism and differential niche utilization in birds. *The Condor*
1020 68:113−151.
1021 Seo T-K (2008) Calculating bootstrap probabilities of phylogeny using multilocus sequence data.
1022 *Mol Biol Evol* 25:960–971.
1023 Shine R (1979) Sexual selection and sexual dimorphism in the Amphibia. *Copeia* 1979:297–306.
1024 Shine R (1989) Ecological causes for the evolution of sexual dimorphism: a review of the
1025 evidence. *Q. Rev. Biol.* 64(4):419−461.
1026 Shultz AJ, Burns KJ (2017) The role of sexual and natural selection in shaping patterns of sexual
1027 dichromatism in the largest family of songbirds (Aves: Thraupidae). *Evolution*
1028 71:1061−1074.
1029 Singhal S (2013) De novo transcriptomic analyses for non-model organisms: an evaluation of
1030 methods across a multi-species data set. *Mol Ecol Resour* 13:403–416.
1031 Stamatakis A (2014) RAxML version 8: a tool for phylogenetic analysis and post-analysis of
1032 large phylogenies. *Bioinformatics* 30:1312–1313.

1033 Starnberger I, Poth D, Peram PS, Schulz S, Vences M, Knudsen J, Barej MF, Rödel M-O, Walzl
1034 M, Hödl W (2013) Take time to smell the frogs: vocal sac glands of reed frogs (Anura:
1035 Hyperoliidae) contain species-specific chemical cocktails. *Biol J Linn Soc* 110:828–838.
1036 Starnberger I, Preininger D, Hödl W (2014) From uni- to multimodality: towards an integrative
1037 view on anuran communication. *J Comp Physiol A* 200:777−787.
1038 Stuart-Fox D, Owens IPF (2003) Species richness in agamid lizards: chance, body size, sexual
1039 selection or ecology? *J Evolution Biol* 16:659−669.
1040 Sztatecsny M, Preininger D, Freudmann A, Loretto M-C, Maier F, Hödl W (2012) Don't get the
1041 blues: conspicuous nuptial colouration of male moor frogs (*Rana arvalis*) supports visual
1042 mate recognition during scramble competition in large breeding aggregations. *Behav Ecol*
1043 *Sociobiol* 66:1587−1593.
1044 Telford SR, Dyson ML (1988) Some determinants of the mating system in a population of
1045 painted reed frogs (*Hyperolius marmoratus*). *Behaviour* 106:265–278.
1046 Telford SR, Passmore NI (1981) Selective phonotaxis of four sympatric species of African reed
1047 frogs (genus *Hyperolius*). *Herpetologica* 37:29–32.
1048 Turelli M, Barton NH, Coyne JA (2001) Theory and speciation. *Trends Ecol Evol*
1049 16(7):330−342.
1050 Veith M, Kosuch J, Rödel M-O, Hillers A, Schmitz A, Burger M, Lötters S (2009) Multiple
1051 evolution of sexual dichromatism in African reed frogs. *Mol Phylogenet Evol* 51:388−393.
1052 Wagner CE, Harmon LJ, Seehausen O (2012) Ecological opportunity and sexual selection
1053 together predict adaptive radiation. *Nature* 487:366−369.
1054 Wells KD (1977) The social behavior of anuran amphibians. *Anim Behav* 25:666–693.
1055 West-Eberhard MJ (1983) Sexual selection, social competition, and speciation. *Q Rev Biol*

58(2):155−183.

Wieczorek A, Drewes R, Channing A (2000) Biogeography and evolutionary history of *Hyperolius* species: application of molecular phylogeny. *J Biogeogr* 27:1231–1243.

Wollenberg KC, Glaw F, Meyer A, Vences M (2007) Molecular phylogeny of Malagasy reed frogs, *Heterixalus*, and the relative performance of bioacoustics and color-patterns for resolving their systematics. *Mol Phylogenet Evol* 45:14–22.

Woolbright LL (1983) Sexual selection and size dimorphism in anuran Amphibia. *Am Nat* 121:110–119.

Yovanovich CAM, Koskela SM, Nevala N, Kondrashev SL, Kelber A, Donner K (2017) The dual rod system of amphibians supports colour discrimination at the absolute visual threshold. *Phil Trans R Soc* 372:20160066.

Zhang C, Sayyari E, Mirarab S (2017) ASTRAL-III: Increased Scalability and Impacts of Contracting Low Support Branches. *Comparative Genomics. RECOMB-CG 2017*. Lecture Notes in Computer Science, vol 10562, eds Meidanis J, Nakhleh L (Springer, Cham), pp 53−75.

FIGURE CAPTIONS

Figure 1. Illustration of ontogenetic color change occurring in hyperoliid frogs (*Hyperolius dintelmanni* shown) that underlies sexual dichromatism. In dichromatic species, females undergo a color change from Phase J to Phase F in response to steroid hormones at the onset of sexual maturity. Males retain the juvenile coloration (Phase J) or undergo a parallel change in color (to Phase F), however the proportion of the male color phases in populations varies across species. Secondary monochromatism can evolve from dichromatism through the loss of Phase J males (both sexes undergo an ontogenetic color change to Phase F) or through the loss of ontogenetic color change in both sexes (both sexes retain Phase J coloration at sexual maturity).

Figure 2. Ancestral state reconstruction of sexual dichromatism in Afrobatrachian frogs from HiSSE using model averaging to account for uncertainty in both models and reconstructions. Circles at tips and nodes are colored by state (yellow: monochromatic, blue: sexually dichromatic), with node pie charts indicating probability of a state assignment. Branches are colored using a gradient from the model-averaged net diversification rate, with black representing the slowest rate and red representing the fastest rate. The arrow highlights the node identified as displaying an unambiguous transition from monochromatism to sexual dichromatism.

Figure 3. The net diversification rate confidence intervals estimated from the best-fit HiSSE model for various combinations of monochromatism, dichromatism, and the presence (+) or absence (-) of the hidden state.

Figure 4. Histograms of the delta AIC comparisons resulting from (A) BiSSE analyses and (B) HiSSE analyses of the 1,500 simulations of neutrally evolving traits on the Afrobatrachia phylogeny. The vertical dotted line represents a delta AIC of two. In the BiSSE analyses (A), delta AIC scores of less than two are considered a failure to reject the 'null' model of constant diversification rates, whereas scores above two for the BiSSE model are interpreted as favoring a correlation between diversification rates and the simulated neutral trait. The HiSSE analyses (B) included five models, but only two were consistently selected as the top ranking, including the HiSSE and CID-4 (character-independent diversification) models. For these analyses delta AIC > 2 was considered as support for a particular model, whereas delta AIC < 2 was considered as equivocal support for the model.

Figure 5. Illustration of (A) several *Hyperolius* species in the predominately sexually dichromatic Clade 1 and (B) several *Hyperolius* species in Clade 2 that exhibit multiple transitions to secondary monochromatism. Females are positioned in the top row, with males below (unless shown in amplexus), and the phylogenetic relationships among species are depicted (though not all species have been included).

1113 **TABLES**

1114 Table 1. Summary of models and fits using hidden state speciation and extinction analyses, with

1115 sexual dichromatism as the observed state. The top ranked model is highlighted in bold.

1116

Description	Model	loglik	AIC	ΔAIC	wtAIC	Hidden States	State-dependent	Net turnover rates	Extinction fraction rates	Distinct transition rates
HiSSE	**19**	**-1033.5**	**2082.9**	**0.0**	**0.445**	**yes**	**yes**	**4**	**1**	**3**
HiSSE	15	-1026.0	2084.0	1.0	0.266	yes	yes	4	4	8
HiSSE	18	-1029.7	2085.4	2.5	0.130	yes	yes	4	1	8
CID-4	14	-1035.3	2086.5	3.6	0.075	yes	no	4	1	3
CID-2	8	-1031.7	2087.3	4.4	0.049	yes	no	2	2	8
HiSSE	16	-1033.5	2088.9	6.0	0.022	yes	yes	4	4	3
HiSSE	25	-1036.1	2092.2	9.3	0.004	only for state 0	yes	3	3	4
CID-4	12	-1035.3	2092.5	9.6	0.004	yes	no	4	4	3
CID-4	26	-1029.7	2093.4	10.4	0.002	yes	no	4	4	9
CID-2	10	-1036.2	2094.4	11.5	<0.001	yes	no	2	1	8
HiSSE	24	-1041.1	2102.3	19.3	<0.001	only for state 1	yes	3	3	4
BiSSE-like	2	-1046.3	2102.6	19.7	<0.001	no	yes	2	1	2
BiSSE-like	1	-1046.3	2104.6	21.7	<0.001	no	yes	2	2	2
BiSSE-like	3	-1053.5	2115.1	32.1	<0.001	no	no	1	1	2
HiSSE	22	-1055.7	2121.5	38.5	<0.001	yes	yes	4	1	3
HiSSE	21	-1053.6	2127.2	44.3	<0.001	yes	yes	4	1	8
CID-4	13	-1060.2	2132.4	49.4	<0.001	yes	no	4	1	1
HiSSE	20	-1061.9	2135.7	52.8	<0.001	yes	yes	4	1	1
HiSSE	17	-1060.4	2138.7	55.8	<0.001	yes	yes	4	4	1
CID-4	11	-1060.4	2138.8	55.8	<0.001	yes	no	4	4	1
CID-2	9	-1068.1	2144.2	61.3	<0.001	yes	no	2	1	1
CID-2	7	-1068.1	2146.2	63.3	<0.001	yes	no	2	2	1
BiSSE-like	4	-1071.4	2152.8	69.8	<0.001	no	yes	2	2	1
HiSSE	23	-1073.9	2153.7	70.8	<0.001	yes	yes	4	1	1
BiSSE-like	5	-1075.2	2158.3	75.4	<0.001	no	yes	2	1	1
BiSSE-like	6	-1077.6	2161.2	78.3	<0.001	no	no	1	1	1

1117

1118

1119 Table 2. Summary of trait rate analyses for the evolution of sexual dichromatism.
1120

Trait Rate Analysis	Log Marginal Likelihood	Transitions 0 > 1	Transitions 1 > 0	Rate Shifts	Rate Minimum	Rate Maximum
Strict Clock Mk1	-92.12	15	7	–	–	–
Strict Clock Mk2	-81.83	2	27	–	–	–
Relaxed Local Clock Mk1	-85.10	16	8	3.3	0.001	0.019
Relaxed Local Clock Mk2	-81.73	2	27	0.8	0.013	0.016

1121 For transition summaries, monochromatism is coded as ‘0’ and dichromatism as ‘1’. The average number of rate
1122 shifts is provided, rather than median.

SUPPLEMENTAL MATERIAL

Figure S1. A species tree of Hyperoliidae inferred from 1,047 gene trees with ASTRAL-III. Node support is shown for quartet support values and multi-locus bootstraps, with branch lengths depicted in coalescent units (except for tree tips, represented by dotted lines).

Figure S2. A chronogram of Afrobatrachia inferred from the multilocus BEAST analysis of 283 species. Taxa labeled with blue color denote the 153 species included in the hyperoliid species tree that was used as a partial constraint tree in this analysis. Node support values are not shown because the tree topology was fixed, but error bars representing the 95% HPD for dating estimates are provided.

Figure S3. A comparison of Bayesian ancestral character reconstructions inferred using the stochastic Mk model of character evolution with symmetrical (Mk1) or asymmetrical (Mk2) transition rates in combination with a strict clock or random local clock model. All analyses enforced a monochromatic root prior. The marginal likelihoods and average number of state changes are shown for each analysis. Node sizes reflect the posterior probability for the inferred character state, and tips and nodes are colored with monochromatism in yellow and dichromatism in blue.

Figure S4. An illustration of transitions to secondary monochromatism inferred using Bayesian ancestral character reconstruction with the Mk2 and strict clock models. Large nodes outlined with red represent inferred transitions to monochromatism from a dichromatic ancestor. States at nodes and tips are colored with monochromatism in yellow and dichromatism in blue.

Figure S5. Ancestral state reconstruction of the observed and hidden state combinations in Afrobatrachian frogs from the best-fit HiSSE model (HiSSE 19; Table 1). Squares at tips are colored by the observed character states (yellow: monochromatic, blue: sexually dichromatic), whereas node pie charts represent the probability of a state assignment to: 1) monochromatism + hidden state absent (yellow), 2) monochromatism + hidden state present (orange), 3) dichromatism + hidden state absent (blue), or 4) dichromatism + hidden state present (purple). No instance of the monochromatism + hidden state present is reconstructed on the phylogeny, whereas a transition to the dichromatism + hidden state present combination is inferred once in the MRCA of two monotypic genera (*Cryptothylax*, *Morerella*), indicating a near absence of the hidden state across the entire tree.

Table S1. Taxon, voucher, and locality information for all samples included in the sequence-capture experiment.

Table S2. A summary of the occurrence of monochromatism and sexual dichromatism in Afrobatrachian species based on literature, museum specimens, and collective field observations.

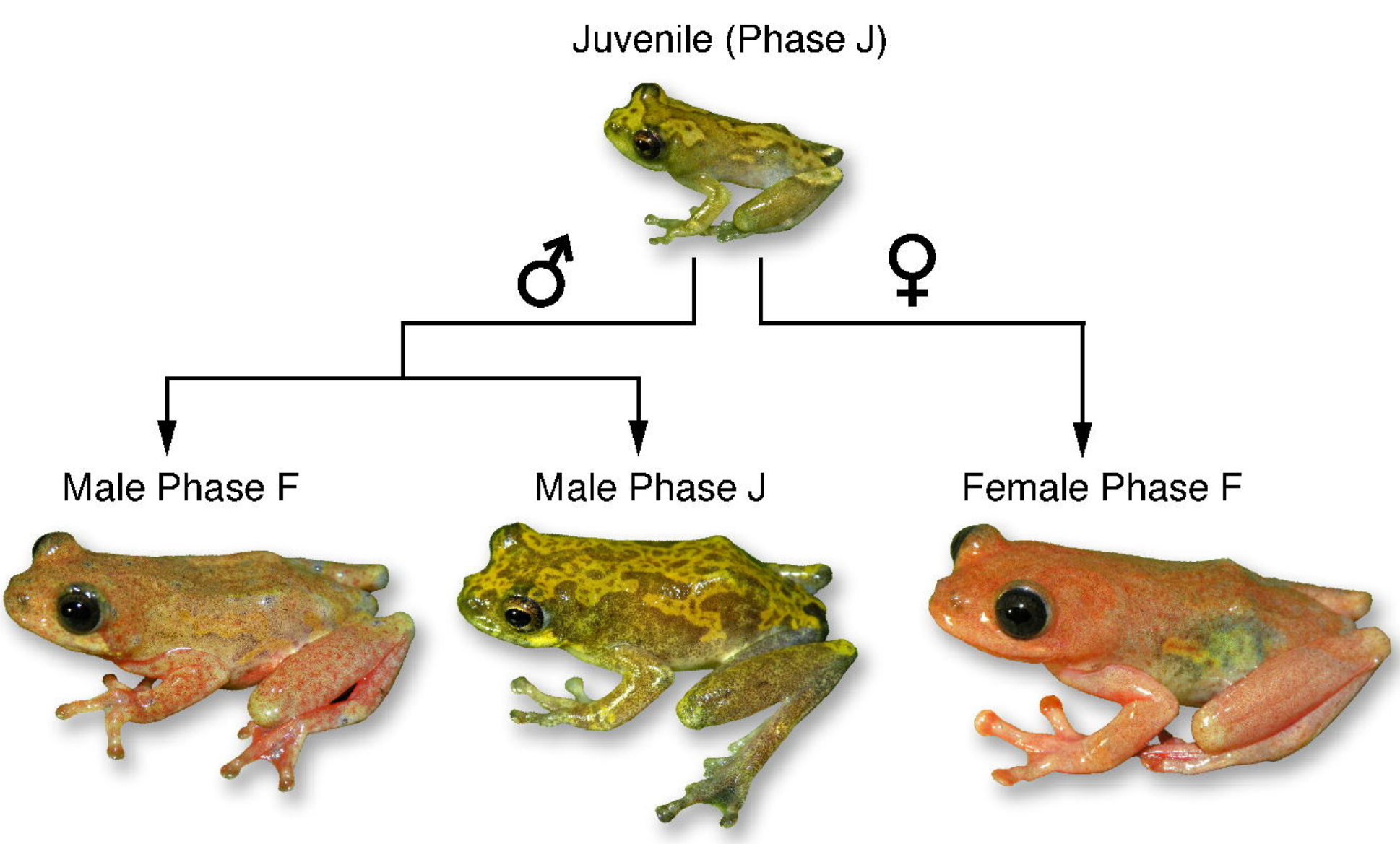
Juvenile (Phase J)
♂
♀
Male Phase F
Male Phase J
Female Phase F

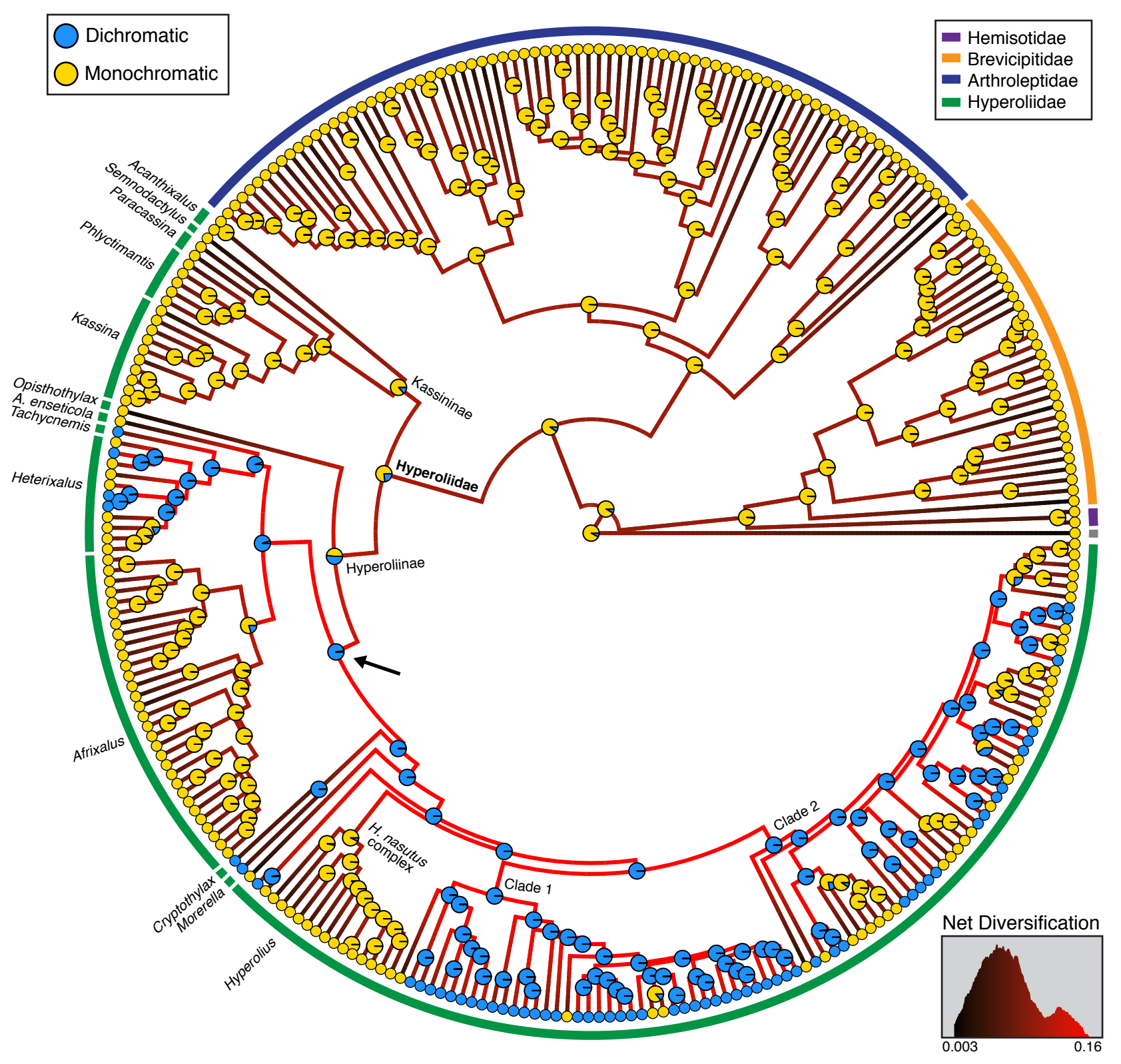
Dichromatic
Monochromatic
Hemisotidae
Brevicipitidae
Arthroleptidae
Hyperoliidae
Acanthixalus
Semnodactylus
Paracassina
Phlyctimantis
Kassina
Opisthothylax
A. enseticola
Tachycnemis
Heterixalus
Afrixalus
Cryptothylax
Morerella
Hyperolius
Kassininae
Hyperoliidae
Hyperoliinae
H. nasutus complex
Clade 1
Clade 2
Net Diversification
0.003
0.16

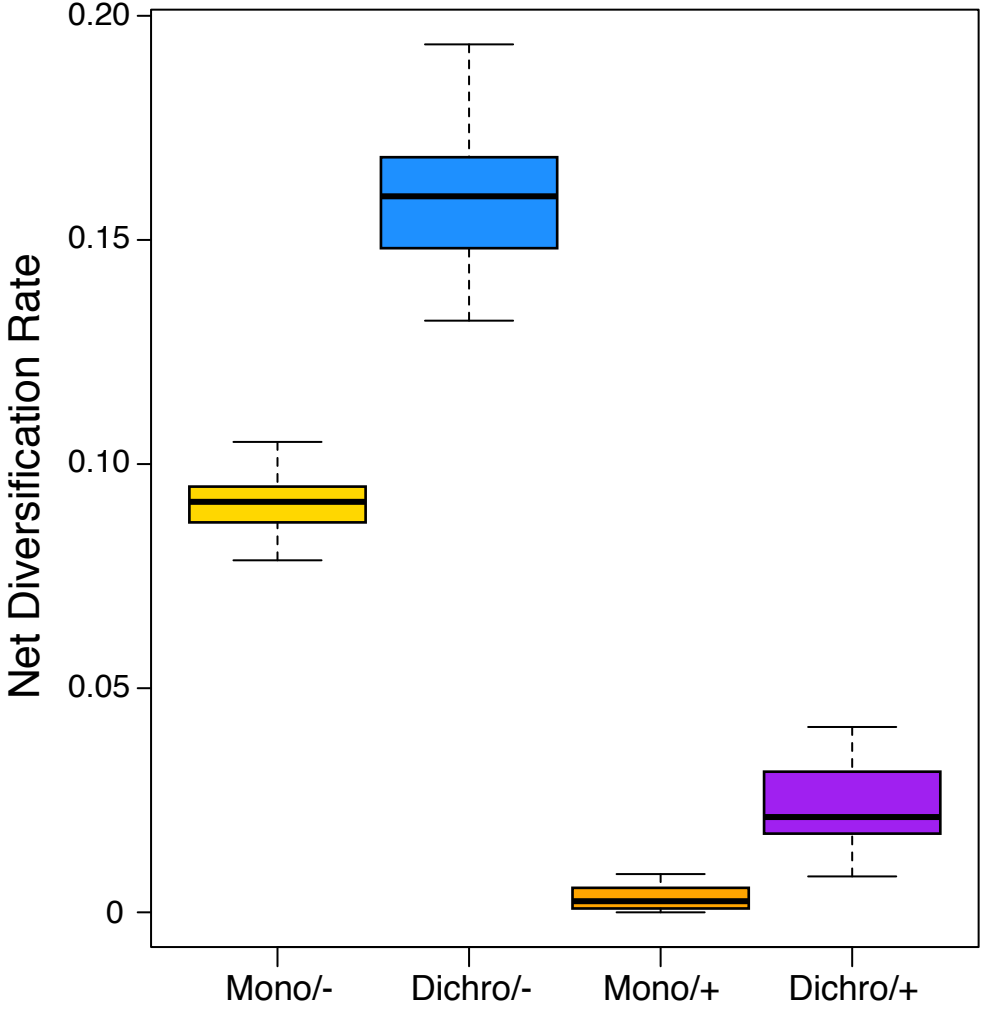
Net Diversification Rate
0.20
0.15
0.10
0.05
0
Mono/-
Dichro/-
Mono/+
Dichro/+

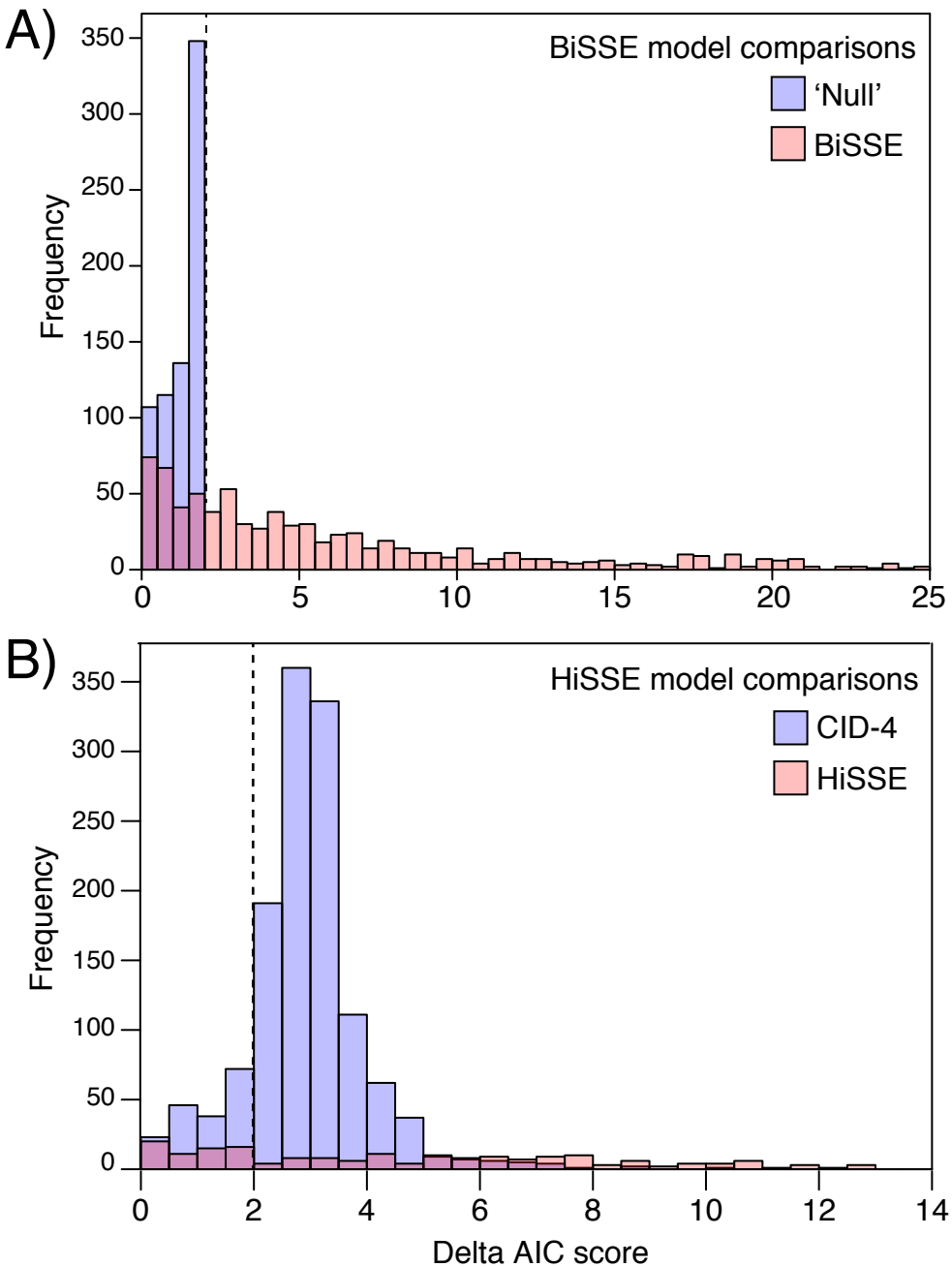
A)
BiSSE model comparisons
'Null'
BiSSE
Frequency
0
50
100
150
200
250
300
350
0
5
10
15
20
25
B)
HiSSE model comparisons
CID-4
HiSSE
Frequency
0
50
100
150
200
250
300
350
0
2
4
6
8
10
12
14
Delta AIC score

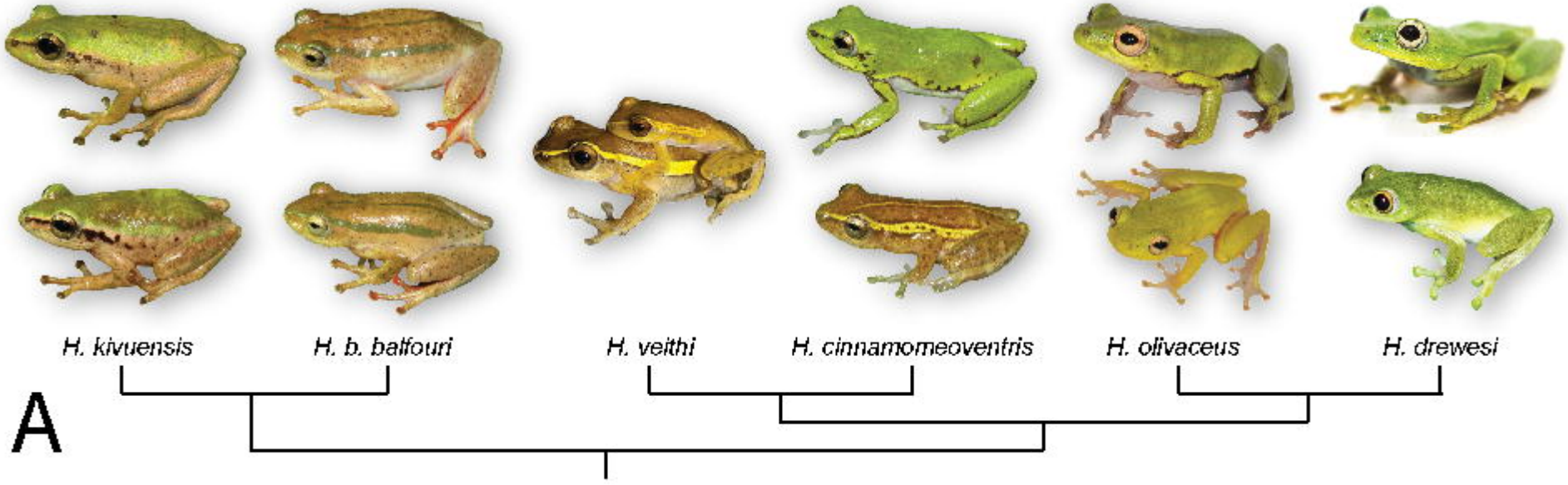
H. kivuensis
H. b. balfouri
H. veithi
H. cinnamomeoventris
H. olivaceus
H. drewesi
A

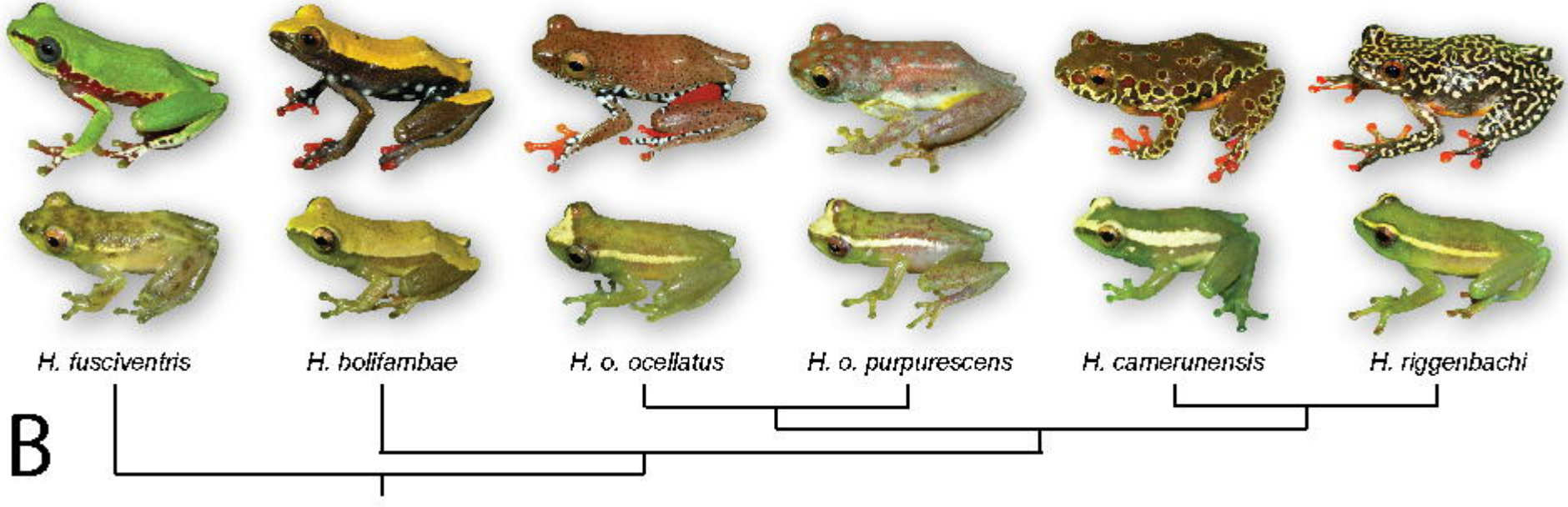
H. fusciventris
H. bolifambae
H. o. ocellatus
H. o. purpurescens
H. camerunensis
H. riggenbachi
B